Molecular switching on surfaces

Steen, Jorn D.; Duijnstee, Daniël R.; Browne, Wesley R.

Published in:
Surface Science Reports

DOI:
10.1016/j.surfrep.2023.100596

Publication date:
2023

Surface Science Reports 78 (2023) 100596

Contents lists available at ScienceDirect

Surface Science Reports

journal homepage: www.elsevier.com/locate/surfrep

Molecular switching on surfaces

Jorn D. Steen, Daniël R. Duijnstee, Wesley R. Browne *

Molecular Inorganic Chemistry, Stratingh Institute for Chemistry, Faculty of Science and Engineering, University of Groningen, Nijenborgh 4, Groningen, 9747, AG, the Netherlands

ARTICLE INFO

Keywords:
Molecular switches
Molecular motors
Surfaces
Interfaces
Spectroscopy

ABSTRACT

Molecular switching has established itself as a key functionality of building blocks developed for addressable materials and surfaces over the last two decades. Many challenges in their use and characterisation have been presented by the wide variation in interfaces studied, these ranging from truly single-molecule devices to two-dimensional self-assembled monolayers and thin films that bridge the gap between surface and macroscopically bulk materials (polymers, MOFs, COFs), and further still to other interfaces (solid–liquid, liquid–air, etc.). The low number density of molecules on monolayer-coated interfaces as well as in thin films, for example, presents substantial challenges in the characterisation of the composition of modified interfaces. The switching of molecular structure with external stimuli such as light and electrode potential adds a further layer of complexity in the characterisation of function. Such characterisation "in action" is necessary to correlate macroscopic phenomena with changes in molecular structure. In this review, key classes of molecular switches that have been applied frequently to interfaces will be discussed in the context of the techniques and approaches used for their *operando* characterisation. In particular, we will address issues surrounding the non-innocence of otherwise information-rich techniques and show how model – non-switching – compounds are often helpful in confirming and understanding the limitations and quirks of specific techniques.

1. Introduction

The field of molecular switches and motors on surfaces and in interfaces is extensive, especially when including such "in-between" systems as metal-organic frameworks (MOFs) and nanoparticles. In this review, we will discuss the various techniques used for characterisation of molecular switching and rotation on surfaces, with a particular focus on the details and peculiarities of each experimental method. For this purpose, we make a selection from published work on various types of surfaces used commonly, and are therefore consciously limiting the scope regarding the vast body of work describing modified surfaces. For further reading, we refer to the reviews mentioned throughout this text that cover particular areas. We will only touch briefly on the use of scanning tunneling microscopy (STM) and spectroscopy (STS) in this field, as a focused review has been published recently [1]. Unsurprisingly, given that surface-confined switching and rotation has clear potential applications, quite a number of reviews in the areas of molecular-scale electronics [2] and control of motion at the nanoscale [3] have been published recently. Furthermore, supramolecular systems were the subject of a recent review by Tian et al. [4], and photo-responsive porous materials, e.g., metal-organic frameworks, covalent organic frameworks, and porous aromatic frameworks by Danowski et al. [5].

A brief introduction is given to molecular switching and the various classes of molecular switches, the techniques used in this area of research, and the types of surfaces that have been studied primarily. In Section 2, we espouse the advantages and drawbacks with the use of individual techniques, in particular regarding their use in the characterisation of molecular switching on surfaces, and common challenges faced when performing these experiments. Section 3 is divided up into sub-sections according to the surface used as substrate for functionalisation with molecular switches or motors with the aim of providing pointers regarding the appropriateness of the available techniques for particular surfaces or interfaces. Section 4 provides a discussion of selected cases that describe in detail the use of a certain technique or combination of techniques to characterise molecular function on functionalised surfaces.

* Corresponding author.
E-mail address: w.r.browne@rug.nl (W.R. Browne).
URL: http://www.brownegroup.eu (W.R. Browne).

https://doi.org/10.1016/j.surfrep.2023.100596
Received 3 November 2022; Accepted 21 February 2023
Available online 9 March 2023

1.1. Molecular switching

Molecular switching is defined here as a large reversible change in structure, and hence properties, of a molecule in response to a stimulus, e.g., electrochemical, thermal, acid-base, or photochemical. In this review, we will limit discussion to systems in which the stimulus leads to a substantial change in molecular structure rather than chromism, e.g., electro- or acidochromism, where only a change in colour (i.e. electronic properties) occurs. Several classes of molecular switches can be defined based on their modes of switching, e.g., *E-Z* isomerisation (stilbene, azobenzene), pericyclic reactions (diarylethene), and pericyclic reactions accompanied by *Z-E* double bond isomerisation (spiropyran) (Scheme 1). As mentioned above, these reversible reactions can be induced by various stimuli, such as, electrode potential, chemical additives, pH jumping, and/or light [6].

Switching of diarylethenes between their open and closed forms involves only a small structural change (and volume of activation), whereas the structural difference between the isomers of spiropyrans (open *vs* closed) and azobenzenes (*cis vs trans*) is larger. The type of molecular switch used to functionalise a surface or interface, therefore, has consequences for the resulting (macroscopic) function, as well as the number of techniques that are available to study its switching.

In this review, however, we have made selections on the basis of the properties of the materials used as substrate, instead of the individual properties of each molecular switch.

1.2. Classes of techniques

Many techniques are now available for characterisation of molecular switching on surfaces, both *in situ* and *ex situ*, most of which are a type of spectroscopy. Absorption spectroscopies make use of a wide range of the electromagnetic spectrum, i.e. X-ray, ultraviolet (UV), visible (Vis), near-infrared (NIR), and infrared (IR). Emission-based spectroscopies are available as well in the X-ray and UV–Vis–NIR region, while Raman spectroscopy is dependent on the wavelength of the laser source (typically 200–1100 nm) and the response of the surface. Several other techniques make use of electron ejection, e.g., X-ray photo-electron spectroscopy (XPS) and high-resolution electron energy loss spectroscopy (HREELS), which, due to the high energy of the irradiation source, are prone to cause irreversible damage to the sample. Whether a technique is destructive or non-destructive depends on the specific situation and not only photon energy – powerful laser sources can also induce thermal damage, for example. Lastly, the use of computational methods is increasing, usually to reinforce the reported experimental observations and proposed mechanisms [7–9], but there are examples also of purely computational investigations into the reactivity and molecular conformations of switches on surfaces [10,11].

1.3. Types of surfaces

The variety of surfaces, interfaces, thin films and coatings that can be formed is immense. Surfaces can be atomically flat [12] or roughened to a wide range of extents, with nanoparticles forming a special category [13–15]; metallic (e.g., gold, bismuth), metalloid (e.g., silicon) [16], fully organic (e.g., covalent organic frameworks) [17], comprised of metal and organic elements (e.g., metal-organic frameworks) [18], and single-molecule [19]. Because of this wide variety, an essentially equally wide variety of methods are used for incorporating switches onto the surfaces and into interfaces (Scheme 2) [20–22]. Molecules can be attached directly to the surface, for instance by vapor or solution deposition onto a substrate, with covalent bonds formed between surface and compound, resulting in an electronically coupled system. Together with a restriction of movement on the surface, this may have consequences for the ability to switch, as we discuss later in this review. Alternatively, an alkyl linker between the molecule and the surface-binding group is often used in the fabrication of self-assembled monolayers to not hamper the switching of the compound by electronically decoupling it from the surface. Regarding the construction of covalent organic frameworks (COFs) and metal-organic frameworks (MOFs), the same limitations need to be taken into consideration. Switches that are part of the backbone or as pendant groups potentially suffer from severely restricted movement, whereas switches absorbed in the pores do to a lesser degree but may instead experience lower stability.

Many surfaces and interfaces have been designed to have certain functions or properties that change upon switching, e.g., electron- and/or proton-conduction, porosity on the nano- or micro-scale, and shape and size of the material [5,23,24]. In this review, instead, we focus on the characterisation of molecular switching, whether this induces a function (on the macroscopic scale) or not.

2. Techniques

In this section, we discuss several key points for each technique in general and, in particular, when applied to (*in situ*) monitoring of molecular switching on surfaces. These points include.

- The information obtained using this technique.
- The description of the surface in the context of this technique, e.g., concentration/surface density, thickness, reflectivity, bulk *vs* surface.
  - For example, regarding UV–Vis absorption spectroscopy, the effective concentration of a compound on a surface is low in comparison to that in solution experiments.

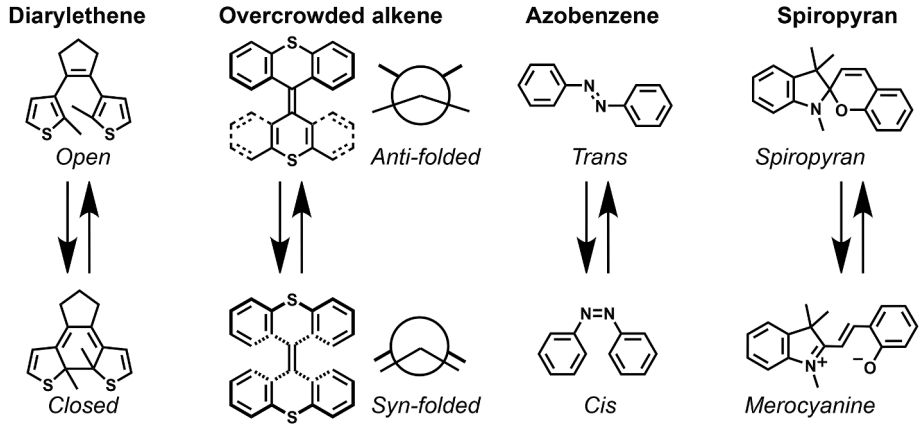

Scheme 1. Selected families of molecular switches and their modes of switching.

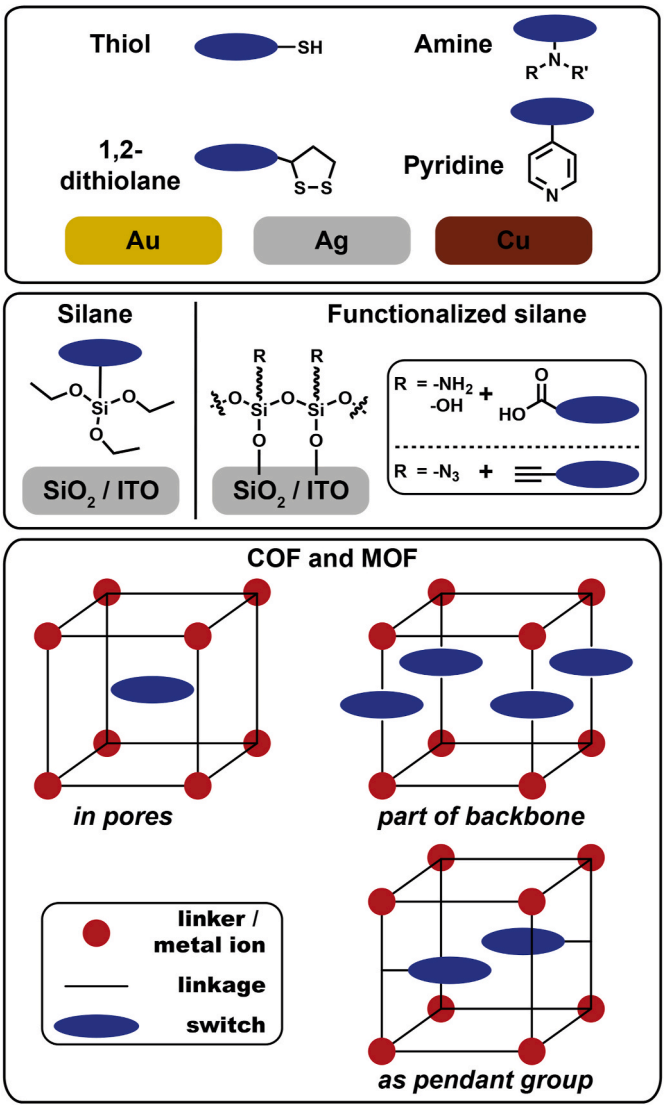

Scheme 2. Strategies for immobilisation of molecular switches onto a surface or in a material: (top) self-assembly of sulfur- and nitrogen-containing functional groups onto gold, silver or copper, (middle) bonding of (functionalised) silanes onto quartz or indium tin oxide, and (bottom) COFs and MOFs where the molecules are absorbed in the pores, are part of the backbone or are present as pendant groups.

- The manner in which the measurement with a technique is performed, and in particular the strengths and limitations of the technique.
- The suitability of the technique for monitoring of molecular switching *ex situ* and/or *in situ*.
  - For photochemical switching: optical access of excitation light source needs to be considered.
  - For thermal switching: thermal effects/artefacts must be considered.
  - For electrochemical switching: access to electrodes, electrolyte (solution), etc.

We will not attempt to cover all aspects of each technique, but rather to provide a succinct description that covers the advantages and disadvantages when applying each technique to the characterisation of switching on a surface, and further reading is indicated where appropriate. Furthermore, optical effects beyond those of molecular origin, e.g., absorption and reflection of light solely determined by the properties of the material that is functionalised, will not be discussed in detail.

There are several common techniques to characterise molecules on surfaces and interfaces [25]. Those that provide vibrational information, such as infrared absorption spectroscopy and Raman spectroscopy, including its variants with enhanced intensity (TERS, SERS, *vide infra*), and those that provide information on electronic properties, such as UV–Vis and NIR absorption spectroscopy. The aforementioned spectroscopies can be applied *in situ* to monitor changes in molecular structure and properties while applying the stimulus required for inducing switching. Other techniques, such as X-ray photoelectron spectroscopy (XPS) and NMR spectroscopy, are typically used *ex situ*, but increasingly *in situ* irradiation is becoming technically feasible. With the *ex situ* approach, spectra are recorded before and after switching. This approach is sensitive to external influences, and to changes occurring to the sample between measurements.

2.1. General phenomena

There are a few general phenomena and potential issues involved with most of the techniques covered here. Molecular switches in pure solid (crystalline) state do not usually show switching behaviour due to restriction of movement in the crystal lattice and inner filter effects, with notable exceptions such as those described by Irie, [26] Uchida [27], and coworkers, for example. Amorphous solids, on the other hand, do not necessarily possess enough space for the molecules to change structure. However, lack of observed switching in this case can often be attributed to the primary inner filter effect (*vide infra*) due to the thickness of the sample. With thin films, full switching in the solid state is often observed [28].

2.1.1. Inner filter effect

The inner filter effect is a common issue in emission-based techniques such as fluorescence and Raman spectroscopy [29]. In the case of negligible overlap of the emission and absorption wavelengths of the system under study, the *secondary inner filter effect*, i.e. the re-absorption of emitted light (e.g., fluorescence, phosphorescence, or Raman scattering), is not of concern. The *primary inner filter effect* can nevertheless still present challenges, particularly at high concentrations, e.g., in NMR photo-isomerisation studies, and at high surface densities, e.g., during irradiation of dense materials such as MOFs [30,31], when the light of a spectrometer or excitation source does not reach the deeper-lying layers of the sample.

The primary inner filter effect is caused by absorption of light by a material, e.g., a MOF, crystal, solution, etc., and is dependent on the molar absorptivity of the material at the wavelength of interest as well as its concentration, following typically the Beer–Lambert–Bouguer law: $-\log(I/I_0) = A = \varepsilon c l = \varepsilon\Gamma$, where ε is the molar absorptivity in $mol^{-1}dm^3cm^{-1}$, c is the concentration in $mol.dm^{-3}$, l is the pathlength in cm, and Γ is the surface density in $mol.cm^{-2}$. The initial light intensity (I_0) is attenuated (to I) with a logarithmic dependence on depth as it passes through the material. Thus, for a typical organic compound (ca. 1 nm long) with a molar absorptivity at a particular wavelength of 10^4 $mol^{-1}dm^3cm^{-1}$ and a surface density of $10^{-10}cm^{-2}$, only 20 monolayers (ca. 20 nm) are required to reduce light intensity at the wavelength to 1% of its initial value. This back-of-the-envelop calculation assumes, of course, that the orientation of the molecules is isotropic, which, for crystals especially, is not the case. The alignment of molecules in non-isotropic environments can mean that the absorptivity is less or greater than the isotropic value and should therefore be taken into account in samples of ultrathin films and (several) monolayers. The effect can also be advantageous though, for example, in multilayer coatings as noted by Feringa et al. recently (Fig. 1) [32].

Experimental methods to correct for the non-linearity of emission intensity with concentration have been developed that make use of calibration with suitable standard samples [33]. Generally, the simplest approach to reduce contributions from inner filter effects is to dilute the

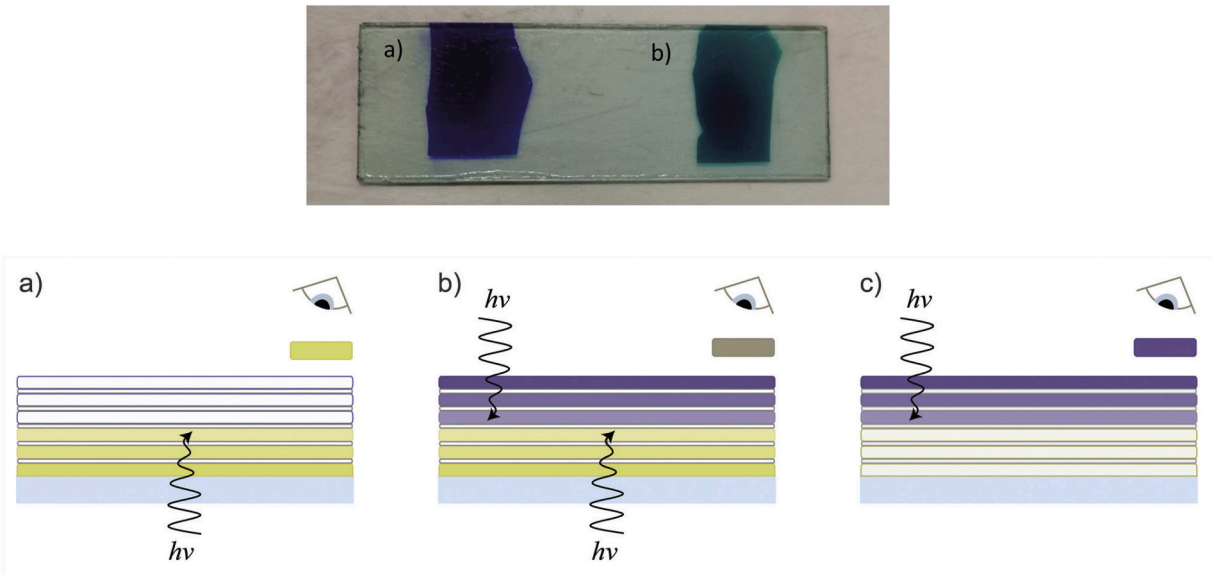

Fig. 1. Glass slides spin-coated with several layers of poly-methyl methacrylate containing either nitrospiropyran (**NSP**) or dithienylethene (**DTE**). (top) Colour obtained upon 365 nm irradiation from the side with **NSP** (a) or **DTE** (b). (bottom) Demonstration of the role of inner filter effect in obtaining multiple colours by selective irradiation of a glass slide coated with multilayers containing two different photochromes. Reproduced from Feringa et al. [32], with permission from The Royal Society of Chemistry. (For interpretation of the references to colour in this figure legend, the reader is referred to the Web version of this article.)

sample, i.e. use a lower concentration or surface density of the compound that absorbs the light. In the case of undesired absorption of Raman scattering by the sample (secondary inner filter effect), either in the initial or in the product state, it may help to choose an excitation light source with a longer wavelength, so as to move further away from the absorption bands of the sample (see also Section 2.4) [34].

2.1.2. Thermal damage

Thermal destruction (known colloquially as "burning") is the damage inflicted to the sample caused by the irradiation source heating it to an extreme temperature (Fig. 2). This is a commonly encountered problem in Raman (micro)spectroscopy due to the use of high power densities, especially with samples of thin films and self-assembled monolayers since the required confocality results in high power densities even with low overall laser power [30,35]. However, even with more sensitive detectors and more efficient optical systems, the effect of sample heating with low power lasers can be surprisingly subtle with relatively modest increases in temperature [30].

2.1.3. Ionisation

High-energy (short-wavelength) spectroscopic techniques, such as any using light in the X-ray region, carry the risk of unwanted ionisation during measurement, which can lead to destruction of the sample. The effect of ionisation can also be highly dependent on the surface, as shown by Ivashenko et al. with comparison of the effect of irradiation on atomically flat and roughened gold surfaces in X-ray photo-electron experiments [36].

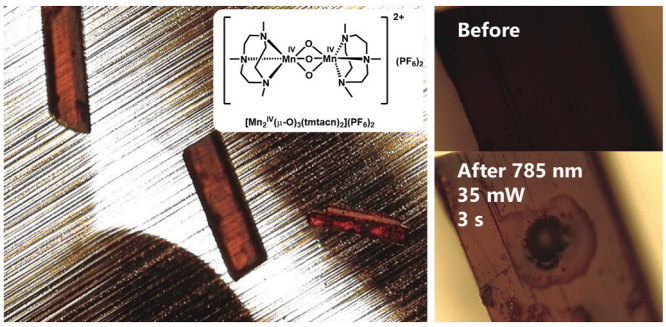

Fig. 2. Crystals of $[Mn_2^{IV}(\mu-O)_3(tmtacn)_2](PF_6)_2$ (melting point >350 °C) before and after irradiation with a 785 nm laser (35 mW, 3 s) during acquisition of Raman spectra, showing thermal damage in the form of a burn region on the crystal. W. R. Browne is kindly acknowledged for providing the images.

2.1.4. Scatter

Scatter by particles of approximately the size of the wavelength of irradiation, i.e. Mie scattering and the Tyndall effect, is a potential issue for absorption spectroscopies in the UV–Vis and NIR regions that obscures the absorption bands of interest [37]. Mie scattering is uncommon in solution studies, unless a reaction produces a precipitate (of the appropriate size), but it is more prevalent in analogous studies on nano- and microparticles. In Raman spectroscopy, the scatter caused by diffuse reflection and specular reflection from reflective surfaces can lead to excessive amounts of stray light swamping the weak Raman scattering signal. In solid samples of powders, the effects of scatter are such as to require integrating spheres to 'catch' the light scattered (see Section 2.2.2).

2.1.5. Optical interference (fringing)

Optical interference, for example fringing, is a phenomenon observed with various techniques but with different underlying causes (Fig. 3). The fringing sometimes observed in UV–Vis absorption spectra is due to the thickness and optical properties of the sample causing interference of the light passing through it by the sample acting as an etalon. Fringing observed in Raman spectra, especially with back-thinned CCDs used for increased sensitivity in the near-infrared region, is due to the thickness of the back-thinned silicon layer approaching the wavelength of light used, and creating an unpredictable etalon and so-called fringing in the image read-out by the CCD. This fringing becomes a 'ripple' in the baseline of spectra with a periodicity often close to the width of vibrational bands.

2.2. UV–Vis–NIR and IR absorption spectroscopy

Absorption spectroscopy has many of the same characteristics as well as limitations in both the UV–Vis–NIR and IR region. When performing absorption spectroscopy of species on surfaces, various aspects need to

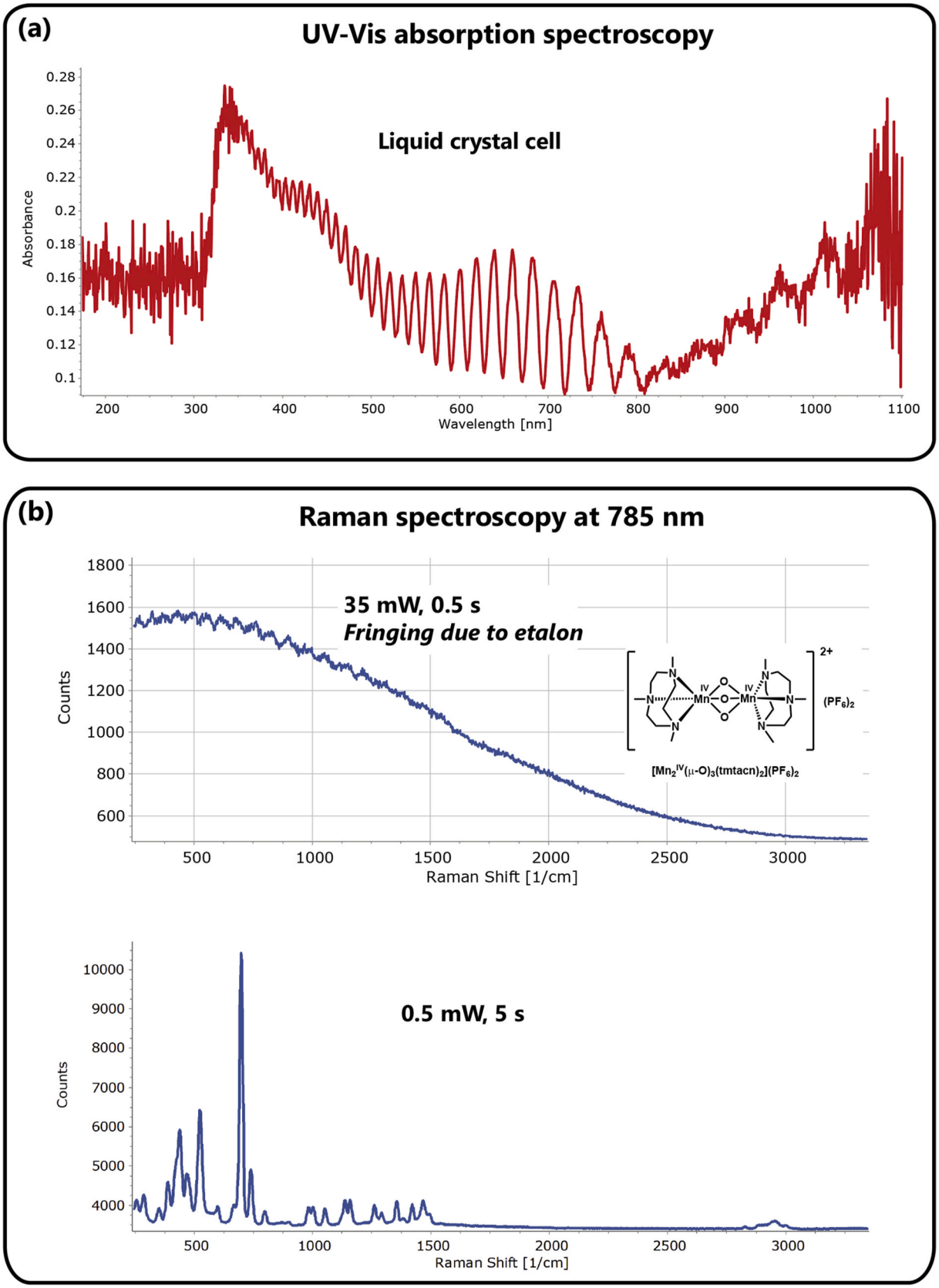

Fig. 3. Fringing in (a) a transmission UV–Vis absorption spectrum of a liquid crystal contained in a cell (5 μm pathlength), and (b) Raman spectra of crystals of $[Mn_2^{IV}(\mu - O)_3(tmtacn)_2](PF_6)_2$.

be taken into account that are not usually encountered in solution. For instance, measurements in transmission mode may not be possible, for example with samples at high concentration (e.g., crystals of MOFs) or on highly reflective or opaque substrates. In these cases, alternative methods, such as the use of reflectance modes and integrating spheres, are more appropriate and will be discussed in more detail in the sections below.

Another phenomenon not encountered in (dilute) solution that has an effect on the absorbance of molecules adsorbed onto a surface is the proximity of those molecules with each other, also called the *solvent effect*, in which molecules act as their own solvent. Furthermore, the effect of macroscopic orientation of chromophores plays a role, where the sample is no longer isotropic and hence the polarisation of the light used to probe the surface becomes an important consideration (*vide infra*) [29]. Similarly, if a high degree of long-range ordering is present, i.e. over the same dimensions as the area of the sample probed, then effects of linear dichroism (LD) can be substantial. While this can be a major problem for circular dichroism (CD) and infrared reflection absorption (IRRA) spectroscopy, it is an extra aspect of interest to study by LD absorption spectroscopy and by polarised Raman spectroscopy.

A perhaps trivial, but nonetheless useful, point, is that the molar absorptivity of a compound, typically expressed in $M^{-1}.cm^{-1}$, can also be expressed in units of $mol^{-1}.cm^2$. Hence, the Beer-Lambert-Bouguer relation, $A = \varepsilon cl$, is also $A = \varepsilon\Gamma$, where Γ is the surface concentration in mol cm^2. A typical value for the molar absorptivity of a layer of organic molecules is around 10^7 mol^{-1} cm^2, and typical surface densities are of the order of 10^{-10} mol cm^{-2} [38]. Hence, the absorbance of a (sub-)monolayer is expected to be of the order of 0.001, and with sufficient accuracy (most higher-end commercial scanning-mode instruments are accurate to 0.0001), surface coverage can be estimated, assuming a reasonably isotropic orientation of the chromophores (*vide infra*).

2.2.1. Transmission spectroscopy

A (metal) surface can be prepared as a film sufficiently thin (approximately 10 nm) such that it is no longer fully reflective and is optically transparent in the near-UV and visible region, making it suitable for use in transmission mode absorption spectroscopy [39–41]. The risk with preparing a layer of metal of only a few nanometers in thickness on a support (e.g., glass or quartz), is that it may not have the properties of a bulk metal due to influence of the surface on atomic packing and the tendency to rearrange thermally to form particles. This is not usually a major consideration as thicknesses of a few nm are already sufficient to overcome the influence of the substrate and, often, a sublayer of another metal is used to stabilize the coating (a chromium interlayer when depositing gold on glass [36], for example). In general, with all surfaces, we have to take into account the unavoidable imperfections and inhomogeneities, such as defect areas.

Regarding absorption spectroscopy in the (near-)infra-red region, the same limitations for transmission mode hold but not necessarily in the same cases as for UV–Vis light. Substrates that do not transmit light in the UV and visible spectrum, and are therefore not suitable for transmission UV–Vis absorption spectroscopy, may be useful for (N)IR vibrational spectroscopy, e.g. silicon. IR absorption by the substrate, solvent, additives, or even strong vibrational modes of the compound of interest, does not necessarily mean that transmission IR absorption spectroscopy cannot be performed. As long as total absorbance of the light is avoided in the region of interest, often where there are characteristic bands of the different isomers of the molecular switch, useful information can be obtained.

The transition dipole moment of a molecule determines the probability of the absorption of a photon [29]. In the case of randomly oriented molecules on a surface, which is usual on the scale of UV–Vis and IR absorption measurements unless the sample is prepared carefully and specifically to obtain alignment, this relation does not pose a problem. If, instead, the functionalised surface is prepared in such a way as to have induced an ordered orientation of the molecules, sample positioning in relation to the incident beam is of influence on the measured absorbance. In the case of randomly oriented molecules on a surface, the molar absorptivity of the compound in solution ($\varepsilon_{solution}$) may be used for characterisation of the adsorbed layer of molecules as well, e.g., to determine the surface density, provided that there is sufficient electronic decoupling from the surface [41].

2.2.2. Diffuse reflectance spectroscopy

Diffuse reflectance spectroscopy requires the dilution (typically <5 wt%) of a solid sample in a non-absorbing, highly reflective powder (e.g., KBr, $BaSO_4$), which, in combination with an integrating sphere, ensures that the light passing through and reflecting from the sample, during which it can also be absorbed, is collected efficiently for detection. Since this measurement requires sample preparation in the form of physical grinding, it is generally unsuitable for surfaces that need to be kept pristine, but is a useful technique for obtaining absorption spectra of more robust materials such as MOFs and nanoparticles [42], especially since samples of these materials can be prepared by drop-casting a concentrated solution in a volatile solvent onto a pellet of, e.g., KBr [28].

2.2.3. Specular reflectance spectroscopy

Specular reflectance absorption spectroscopy makes use of highly (specular) reflecting substrates. The incident light passes through the absorbing layer on top of the substrate. Since the substrate only needs to be reflective in the spectral region of interest, it can be used for vibrational spectroscopy even when UV and visible light is absorbed, and *vice versa*. There are two main methods which are distinguished by the thickness of the layer on the reflective substrate [25]. Specular reflectance is used when the layer is sufficiently thin that the path of light is undisturbed. At the other end, when the layer is thicker and the path of light is changed due to its difference in refractive index, it is called reflection absorption spectroscopy. The latter is widely applied to obtain vibrational spectra of solids and surfaces, and is aptly called infrared reflection absorption spectroscopy (IRRAS). When polarisation modulation of the incident light is used as an extra parameter, the technique is called PM-IRRAS [43]. The advantages of this latter approach are reduced acquisition times, the absence of significant disturbances by the environment, and the fact that recording of a background signal is unnecessary [44]. Various sampling methods are used to record IRRA spectra, for example, with a single-reflection horizontal ATR accessory on a regular FTIR instrument [43], or in grazing-incidence reflection mode where the angle of incidence with the surface normal typically is 80° [45,46].

2.2.4. Technique-specific aspects in relation to photochromic switching

2.2.4.1. UV–Vis–NIR absorption spectroscopy. Molecular switches and motors that exhibit a significant change in their electronic absorption spectrum upon applying a correct stimulus, i.e. chromism, are suitable for study by UV–Vis–NIR absorption spectroscopy. In the case of photochromes, it is important to note that photochemical switching can also occur due to the radiation from the lamps of the spectrometer used to acquire spectra, and care must be taken to avoid this as much as possible, e.g., by using a shutter to block the light in-between acquisitions or a filter to block light except in the region of interest. The families of spiropyrans (and spirooxazines) and azobenzenes are prime examples of switches well-suited for monitoring by UV–Vis absorption spectroscopy because of the clear differences in visible absorption between the spiro and merocyanine isomers [47], and the *cis*- and *trans*-isomers, respectively [40]. The electronic absorption properties of a switch can be useful also for Raman spectroscopy, in obtaining so-called resonantly enhanced Raman spectra, which will be discussed in more detail in Section 2.4.1.

2.2.4.2. FTIR absorption spectroscopy. FTIR absorption spectroscopy provides structural information on the surface-bound molecules, but unlike Raman spectroscopy (*vide infra*), the infrared light of the irradiation source does not interfere with the measured signal, nor does it induce photochemical switching. A shared issue, however, is heating of the sample under study due to non-radiative relaxation from a vibrationally excited state. Furthermore, for Attenuated Total Reflectance (ATR) mode, there is a wavelength-dependent limit to the sample thickness that can be used, with a greater penetration depth at lower wavenumbers [48,49], and transmission mode and IRRAS are often the methods of choice.

Having a characteristic band, with which to follow switching, that appears only in the FTIR spectrum of one isomer, is generally guaranteed when a large change in molecular structure occurs, since the vibrational spectrum itself is a manifestation of the shape and symmetry of the molecule. An example is found in the work by Tuczek et al. on azobenzene-functionalised triazatriangulene platforms onto which a methoxy unit was installed that functions as a marker group [44]. With this, the *cis-trans* isomerisation of the azobenzene platform immobilised on Au(111) is readily discerned, allowing for it to be shown that the isomerisation back to the initial state is significantly faster on the surface than in solution.

2.3. Emission spectroscopy

Emission in the near-ultraviolet and visible region of the spectrum, e.g., phosphorescence and fluorescence, is in principle a zero-background technique, and therefore emission is readily detected over the background noise (electronic and shot noise, primarily). Of course, in order to be a useful technique for monitoring of switching, either only one of the states of the switch should be emissive, or both but each with emission of different wavelengths. Emission spectroscopy in the X-ray region of the electromagnetic spectrum will be discussed in Section 2.8.

Emission spectroscopy is a central technique in so-called single-molecule studies, with a recent Nobel prize awarded for the super-resolution microscopies [50], which make use of the 'blinking' of isolated molecules, but it is also useful in the study of monolayers. Coleman et al. used the distinct fluorescence spectra of bistricyclic aromatic enylidene (BAE)-based fluorophores to follow the photo-induced reaction in which a blue-emitting BAE acting as an energy donor was converted *in situ* photochemically to a green-emitting BAE acting as an energy transfer acceptor on an indium tin oxide-coated glass substrate [51]. While this example does not involve reversible switching, it shows clearly that emission spectroscopy is useful in determining when a reaction occurs from one fluorescent compound to another, and in this case the corresponding absorption spectra revealed limited switching of the system due to the energy transfer quenching induced by the photo-product. The main challenge in using emission as the molecular property for characterising monolayers and thin films, is that even relatively stable compounds are prone to irreversible photodamage under continuous irradiation due to low quantum yield photo-degradation processes. Furthermore, the approach is generally limited to systems with a reasonably high emission quantum yield.

2.4. Raman spectroscopy

Raman spectroscopy, an emission-based technique also, does not require the recording of a reference signal, as opposed to absorption spectroscopies [34,52]. Therefore, its advantage lies in samples that suffer from irregular changes in optical properties, for instance in the case of samples that are sensitive to small changes in position. Raman scattering obtained from a sample provides molecular vibrational information, but is sometimes used to detect lower-frequency lattice modes as well (e.g., phonons). Since the intensity is proportional to the fourth power of the frequency of excitation, generally it is best to use a laser with as high a frequency as possible. However, using a laser of a wavelength in the UV and visible region increases the risk of interferents such as fluorescence background signal and the primary and secondary inner filter effect, due to electronic absorption by the sample in this region. Excitation wavelength and sample concentration are two factors that can be adjusted to some extent. Changing the laser source is relatively straightforward, provided that multiple lasers are available to the experimentalist, but can cause several issues as well, as discussed below. For Raman spectroscopy on functionalised surfaces, the main limiting factor is the concentration, since it may be challenging to increase concentration or surface density of a sample without changing the chemical behaviour.

Analogous with the dependence of electronic absorption on the transition dipole moment of molecules immobilised on a surface, Raman scattering intensity is polarisation-dependent. In the case of highly oriented surfaces (e.g., thin films of crystals and MOFs [30]), the acquired spectrum will depend on the orientation of the molecules with respect to the laser, manifested in a change in ratio of polarisation-sensitive vibrational modes. On the other hand, polarised Raman spectroscopy can be used as an additional characterisation technique as well [30].

As discussed in Section 2.1.2, Raman measurements are particularly prone to inducing thermal damage of the sample because of the high laser power densities applied. In the case of surfaces functionalised with molecular switches, a related problem, though typically not irreversible, is thermal switching of the molecule on the surface [53,54]. Both of these phenomena, thermal damage and thermal switching, are still possible when using a laser wavelength outside of the range of electronic absorption by the sample, since near-IR light (>800 nm) can be absorbed by overtones of vibrational modes as well. Furthermore, photochemical switching with a highly focused near-IR laser has been shown to be possible as well due to two-photon absorption [55]. This may be avoided readily by reducing the power output of the excitation laser as two-photon processes have a quadratic dependence on laser power (see Section 4.3).

Another issue commonly encountered in the acquisition of Raman spectra is emission, e.g., fluorescence and phosphorescence, that appears as a broad background signal and can thereby swamp the lower-intensity Raman bands due to the increase in shot noise. When the emission originates from the molecular switch (before and/or after switching), this will usually preclude the use of Raman spectroscopy for characterisation, but also impurities present in the sample, even in tiny amounts, can pose a problem when their quantum yield of emission is significant. In case of fluorescence background intensity, the severity of this may be avoided by choosing either a longer wavelength of excitation, such that the part of the electromagnetic spectrum observed lies beyond that where fluorescence is observed (Fig. 4), or even a shorter laser wavelength, so as to avoid detecting the longer-wavelength fluorescence. Two-photon excitation of fluorescence is less common, but can also prevent the recording of Raman spectra at any wavelength [56].

It follows from the potential issues presented above that Raman spectroscopy is not necessarily an innocent technique. However, several methods can be used in order to prevent undesired side effects from laser-induced heating, such as using low laser power, and immersion/dispersion of the sample in a solvent to improve heat dissipation.

2.4.1. Resonance enhancement of Raman scattering intensity

When the Raman intensity in a non-resonant Raman measurement is insufficient for detection, there are several ways to achieve enhancement of the signal. Although electronic absorption by a sample poses a possible problem, one can take advantage of this property as well by choosing an excitation source at a wavelength where there is an absorption band, and hereby obtaining resonance enhancement of the Raman scattering intensity (Fig. 5) [58–61]. Inherent to this enhancement is also the greater risk of thermal damage to the sample.

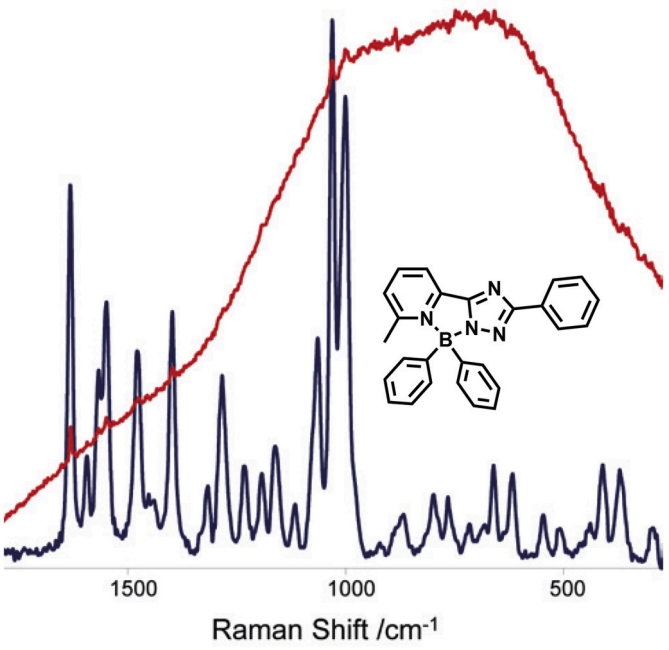

Fig. 4. Solid-state Raman spectra of a boron complex at 785 nm showing its intense fluorescence background (red), and at 1064 nm in which fluorescence is completely absent (blue). Adapted from Browne et al. [57] (For interpretation of the references to colour in this figure legend, the reader is referred to the Web version of this article.)

2.4.2. *Surface-enhanced Raman scattering and tip-enhanced Raman scattering spectroscopy*

Surface-enhanced Raman spectroscopy [62] (SERS) and its variant tip-enhanced Raman spectroscopy [63,64] (TERS) have been used extensively in the characterisation of molecules adsorbed on surfaces. A notable phenomenon associated with SERS is the fact that a large portion of the overall surface-enhanced intensity is contributed by a small percentage of total sites on a surface: so-called "hot spots" [65,66].

The experimental setup for a SERS measurement is largely the same as for regular Raman spectroscopy. Specific requirements and challenges will depend on the sample being studied, e.g., nanoparticles or a roughened planar surface.

A TERS instrument combines a Scanning Tunneling Microscope (STM) with a Raman spectrometer in order to obtain Raman spectra of molecules on the probed surface at the STM tip (Fig. 6). In theory, TERS makes it possible to track atomic changes simultaneously with changes in vibrational frequencies. In a review, not specifically related to molecular switching, Deckert-Gaudig et al. discuss the history and experimental details of the technique [64]. Importantly, the enhancement of Raman scattering is due to the STM tip – indeed, the probed surface does not need to be rough, as is the case with SERS, and this allows for the study of atomically flat surfaces with high spatial resolution using TERS [39]. As with other vibrational spectroscopic methods, the application of TERS spectroscopy is most useful when a characteristic Raman band of at least one isomer of the molecular switch is known, for instance, in the case of hydrazone-based photoswitches [39] and azobenzenes [67]. Unfortunately, it is experimentally challenging to irradiate a sample during acquisition of TERS spectra, and hence generally only the situations before and after irradiation can be characterised.

A phenomenon that needs to be taken into account when using the resonance enhancement from surface plasmons is plasmon-driven chemical reactivity [65]. This topic will be discussed in more detail in Section 4.2. An undesired consequence of using an STM tip that is made of (reactive) metal, usually silver, is attachment of molecules originating from the functionalised surface under study. Lee et al. noted this effect when chemisorption of a single molecule of a thiol-substituted azobenzene derivative onto the silver STM tip resulted in its observation by TERS, while the molecules adsorbed onto the gold substrate were not detected due to their flat orientation on the surface [68].

Single-molecule SERS is a relatively new technique that can be used to follow photochemical reaction events of, for example, molecular switches [69]. It should be noted that the measurement interferes significantly with the molecule under study. Oftentimes, intensity fluctuations are observed in these types of single-molecule Raman spectroscopic experiments which may be due to changes in diffusion, adsorbate-substrate orientation, or local electromagnetic field gradients, but may also rather be the result of more subtle variations in the lifetime, energy, and geometry of the excited state, as concluded by Van

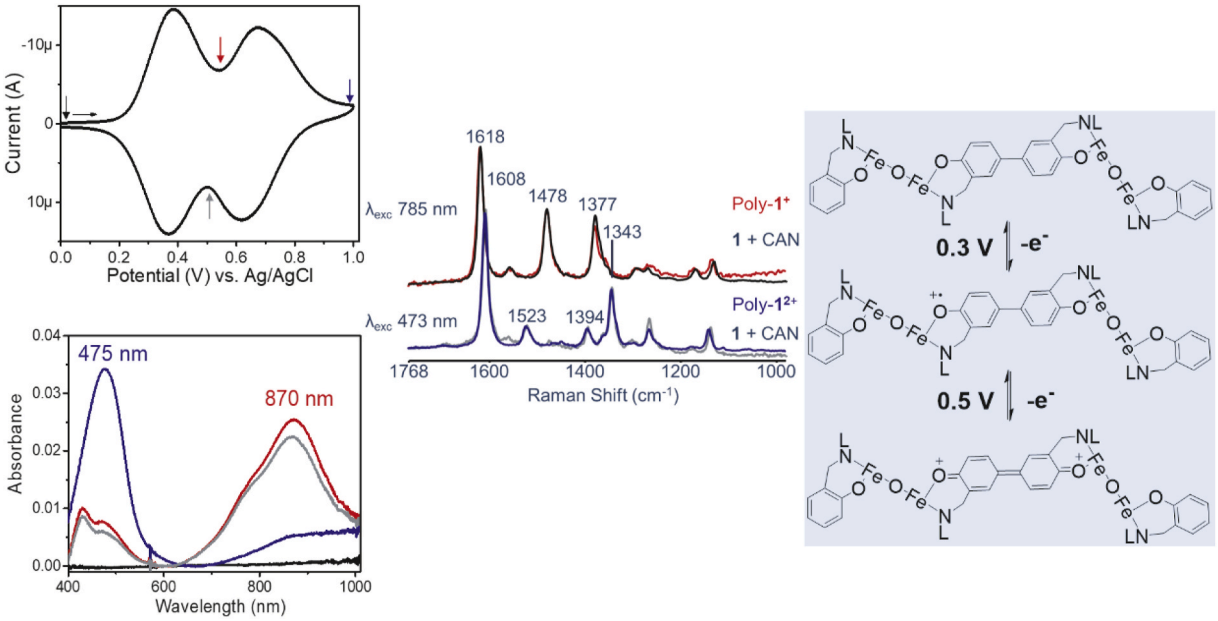

Fig. 5. Cyclic voltammetry and Raman spectra of a thin film (1–2 nm) of an electrochemically polymerized Fe(III)-polypyridyl complex, with resonance enhancement of the singly oxidized polymer at 785 nm and of the doubly oxidized polymer at 473/488 nm. Reproduced from Unjaroen et al. [60], with permission from the American Chemical Society.

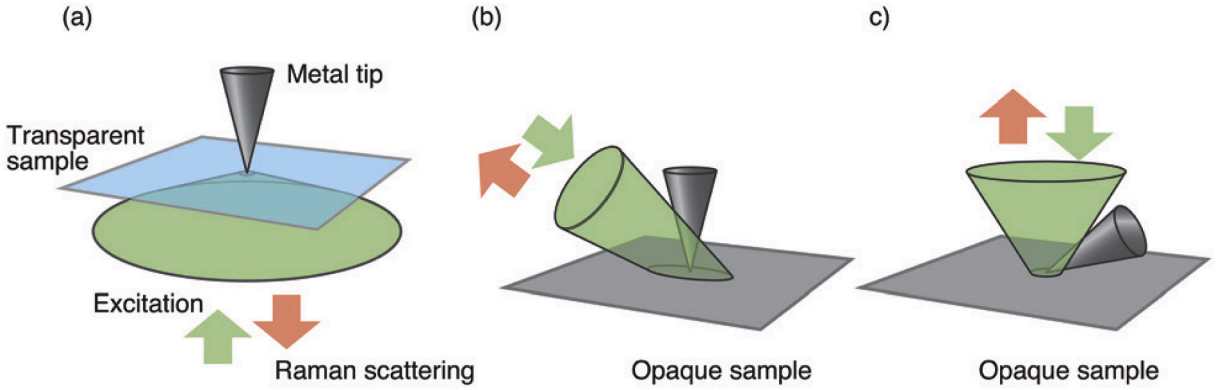

Fig. 6. Experimental arrangements for TERS: (a) back-reflection with illumination from the bottom (limited to transparent substrates only), (b) illumination from the side, and (c) illumination from the top. Reproduced from Deckert-Gaudig et al. [64], with permission from The Royal Society of Chemistry.

Duyne et al. from theoretical calculations [70].

2.5. High Resolution Electron Energy Loss Spectroscopy

High Resolution Electron Energy Loss Spectroscopy (HREELS) is a surface-sensitive technique that is distinct from the other spectroscopies discussed here in that it utilises a monochromatic electron beam to measure the energy loss of electrons undergoing inelastic scattering on a surface, hereby providing vibrational information of the adsorbed molecules on that surface [71]. Since ultra-high vacuum conditions are required, and the surfaces that can be studied are limited to relatively smooth and crystalline materials, HREELS has limited applicability and requires specialised instrumentation that is not readily available. Although most of the commonly desired (vibrational) information of the adsorbate can be obtained by FTIR and IRRA spectroscopic methods, there is certain information that only HREELS can provide, i.e. particular surface processes that can be observed with electrons since the selection rules are different for scattering of electrons than for vibrational absorption of light. The technique is reviewed by Tegeder in regard to photochemically- and thermally-induced molecular switching on noble metals [20].

2.6. Localised surface plasmon resonance spectrosopy and ellipsometry

Both localised surface plasmon resonance (LSPR) spectroscopy and ellipsometry are techniques that provide information about the properties of the surface, and only indirectly of the molecules adsorbed onto it, and therefore do not give direct insight into molecular changes that occur during switching. Ellipsometry is widely used to study the dielectric properties of thin films [72], whereas LSPR spectroscopy gives insight into the surface plasmon of nanoparticles with sub-wavelength spatial resolution [73,74].

2.7. Non-linear optical spectroscopies

The main distinct feature of non-linear optical (NLO) spectroscopy that gives it an advantage over linear optical techniques, is that the signals can only come from the surface or interface since these are never centrosymmetric – a requirement for obtaining non-linear optical effects [75]. Sum-frequency generation (SFG), second-harmonic generation (SHG), and two-photon photo-emission (2PPE) spectroscopy are a few of the most commonly used NLO techniques, and their use for characterisation of molecular switching on noble metals is discussed in the review by Tegeder [20].

Sum-frequency generation (SFG) vibrational spectroscopy, also called vibrational sum-frequency (VSF) spectroscopy, offers a significant increase in spatial resolution compared to other vibrational spectroscopies, such as IRRAS, since the signals that are recorded have to come from molecules that are on the surface [76]. Because of this property, SFG vibrational spectroscopy has been shown to give more detailed information of molecular structure on surfaces, as demonstrated by Ye et al. in the determination of the orientation of the nitro group of a nitrospiropyran-functionalised gold surface in both the open and closed form [77]. In addition, the technique was used to obtain the photo-isomerisation rate on the gold surface for comparison with those in solid state (lower) and in polar solvents (same). Photo-switching studies of azobenzene SAMs on gold using the same technique allowed Tegeder et al. to draw the conclusion that the mechanism of photo-isomerisation of azobenzene SAMs is analogous to that of free molecules in solution, namely direct electronic excitation [78]. An interesting example of the combination of this spectroscopic technique with electrochemistry is the investigation by Garling et al. into the influence of surface potential on the photo-switching of a nitro-substituted spiropyran SAM on gold [79]. Tegeder et al. applied second harmonic detection in the characterisation of switching, when observing that the generation of second harmonics by fulgimide molecules self-assembled on Si(111) happens to varying extents dependent on the particular isomers present on the surface [80]. Another example of the use of NLO spectroscopic techniques by the same group is the detection of two-photon photo-emission signals of spiropyran and merocyanine deposited on Au(111) to probe the molecular orbital energies of the states of the molecular switch [81]. For spiropyrans adsorbed directly onto a surface, the quantum efficiency for ring-opening was found to be several times lower than that in solution, which is explained by the efficient quenching of excited states by the metal surface.

As with other vibrational spectroscopic techniques, it is of great practical use for the molecules under study to exhibit characteristic spectral bands, ideally in both states of the molecular switch. The above-mentioned reports show that the nitro-substituted spiropyran has ideal marker bands originating from the nitro group, hence its ubiquity in the literature. Both the symmetric and asymmetric stretching modes are present in spectra of both the closed spiropyran and open merocyanine isomer [79], which facilitates determination of the extent of switching on surfaces.

2.8. X-ray spectroscopies

2.8.1. X-ray photo-electron spectroscopy

X-ray photo-electron spectroscopy (XPS) provides information on the oxidation state and bonding interactions of atoms in the molecule on a surface (Fig. 7) [82,83]. There is a risk of damage to the sample during measurement, as well as undesired reactivity due to the experimental conditions of the XPS instrument, which will be discussed in Section 4.3. A downside to XPS in the characterisation of photochemical switching is that it is experimentally challenging to perform *in situ* irradiation during a measurement, which means typically that samples are characterised

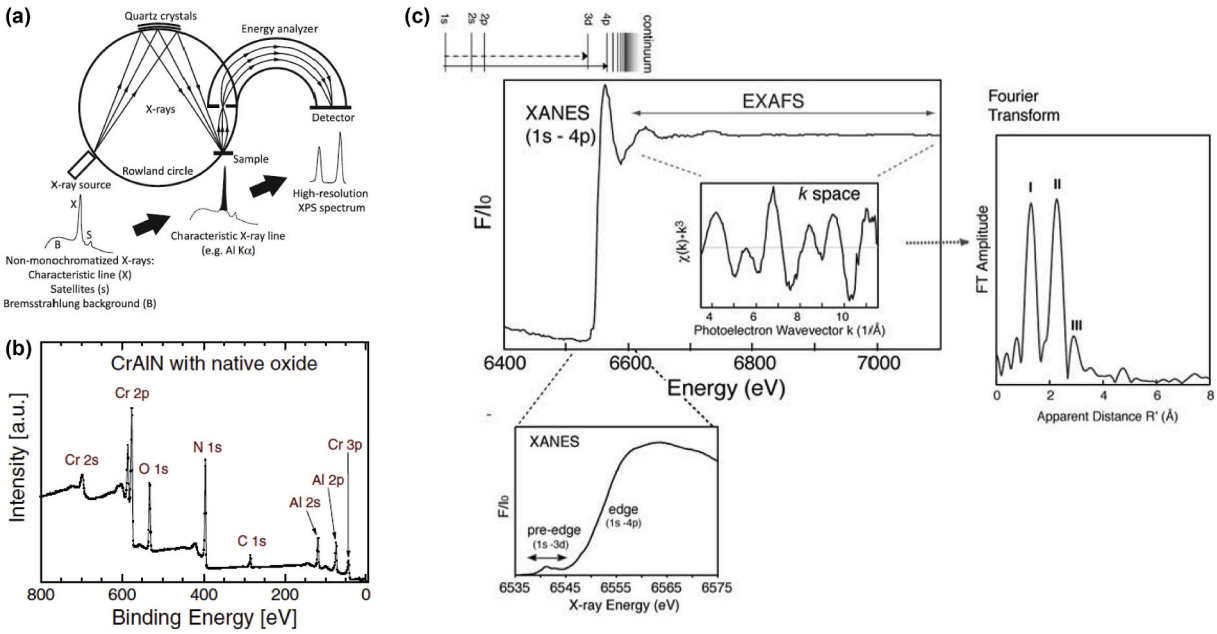

Fig. 7. (a) Schematic illustration of an X-ray photo-electron spectrometer with a monochromatized X-ray source and hemispherical electron energy analyzer, and (b) an example of a wide-range XPS spectrum of a thin film of CrAlN with a native oxide layer. Adapted from Greczynski and Hultman [83], with permission from Elsevier B.V. (c) X-ray absorption spectrum of Mn showing the different regions: K-edge XANES, and *k*-space EXAFS with its Fourier transform. Adapted in part from Yano and Yachandra [85], with permission from Springer Nature.

by recording of spectra before and after irradiation. Furthermore, the technique has a steep depth sensitivity of less than 5 nm [84], making it challenging to accurately interpret data for high-density SAMs and thin films. A further challenge is electrical charging of the substrate [83]. Using conducting substrates and an electron gun can reduce these effects.

2.8.2. *X-ray absorption spectroscopy*

An X-ray absorption spectrum includes a wide range of energies where the various regions contain different types of information (Fig. 7). Commonly, the part of the absorption spectrum near the edge structure is focused on with a technique called both X-ray absorption near-edge structure (XANES) and near-edge X-ray absorption fine structure (NEXAFS) [86]. The complementary technique extended X-ray absorption fine structure (EXAFS) is used to study the fine structure in the absorption at energies higher than that needed for electron release, in this way reporting on the nature of the neighbouring atoms and their distance from the absorbing element [85]. While for certain measurements the high noise level associated with in-house NEXAFS instruments is an obstacle that can be overcome, most samples require access to synchrotron facilities, at least those in low concentration.

NEXAFS data can give clear information on the switching on surfaces of, e.g., rotaxanes, as shown by Schalley et al. on gold for which chloride ions were used as stimulus (i.e. chemical switching) [87], but often the differences before and after switching are more difficult to determine, as with the photo-switching of azobenzene deposited on semi-conducting HfS_2 and metallic $TiTe_2$ [88]. XPS spectra also clearly indicated a change in the carbon and nitrogen atoms of the deposited azobenzene, while the differences in NEXAFS spectra before and after irradiation were minor. The tilt angle of the azobenzene changed after irradiation [86], and this reduction in NEXAFS polarisation contrast is interpreted as evidence of photochemical switching of azobenzene adlayers [89]. When the same measurements were performed for monolayers of azobenzene instead of multilayers, the tilt angles could not reliable be obtained due to an insufficient signal-to-noise ratio. This shows that NEXAFS requires a certain surface density of samples in order to permit satisfactory interpretation and is therefore not suitable for monolayers.

2.8.3. *X-ray emission spectroscopy*

An alternative way to obtain an X-ray absorption spectrum is to employ X-ray emission spectroscopy (XES) and emission-detected X-ray absorption to generate an excitation spectrum similar to that done in the UV–Vis spectral region [90,91]. It is widely used in X-ray spectroscopy and is particularly useful when sample absorption is too high and it is experimentally challenging to obtain an X-ray absorption spectrum directly.

2.9. *Nuclear magnetic resonance spectroscopy*

Nuclear magnetic resonance (NMR) spectroscopy has been used for the characterisation of nanoparticles functionalised with a molecular switch [92], and for determining the unidirectionality of the photochemically-driven rotation of a molecular motor on gold nanoparticles using a ^{13}C-labelled analogue [93], albeit not *in situ* but by recording of NMR spectra after cleavage from the gold surface. In recent years, solid-state NMR spectroscopy has gained increasing interest as a tool for characterisation of a wide range of materials [94], for instance metal-organic frameworks, for which it was demonstrated to be a useful probe of the dynamic processes occurring inside of a framework containing mechanically interlocked molecules [95].

2.10. *Computational chemistry*

Computational chemical methods are often used in addition to experimental work as an aid to explain observations [7–9], in particular when dealing with complicated measurements whose results pose a challenge for interpretation, such as X-ray-based spectroscopic techniques.

Simulations of X-ray absorption spectra of diarylethene on highly-oriented pyrolytic graphite (HOPG) using density functional theory (DFT) have helped identify the isomers present before and after photo-isomerisation [96], and the surface coverage- and temperature-dependent conformations of an imine switch on Au(111) were computationally investigated by first-principles DFT calculations to help explain the changes observed by NEXAFS [97]. The surface

coverage dependence of the excited-state properties of adsorbed azobenzene was rationalised by Cocchi et al. who reported that high-density architectures show almost no π-π^* resonance, which is the excitation that triggers *cis-trans* isomerisation, whereas this is observed in the computed optical spectra of isolated dimers and diluted self-assembled monolayers [98,99].

There is usually a disparity between calculations that use molecular models to describe functionalised surfaces, and observations from experimental work, more so than is the case for molecular systems such as gases and solutions. A periodic approach to model surfaces and complete substrate-adsorbate systems can be taken, e.g., the Vienna *ab initio* simulation package (VASP) based on DFT [100,101]. Nevertheless, Balema et al. have used gas-phase DFT calculations with simplified models of metal-organic complexes to predict preferred molecular orientation on a Cu(111) surface, by comparison of methoxy- and ethyl-substituted adsorbates that show different orientation of their side groups [102].

Kshirsagar et al. studied the optical absorption of an azobenzene-functionalised metal-organic framework computationally and found that the simplest model could describe nearly all of the ultraviolet and visible absorption bands [103]. The noticeably strong S_1 absorption band of the *cis*-isomer, that was only correctly described by larger models, indicates at the same time that azobenzenes embedded in the modelled framework should have a higher rate of *cis-trans* isomerisation than in solution. This theoretical work holds implications for the design of azobenzene-functionalised MOFs aimed to have high photo-conversion efficiencies.

Theoretical studies of molecular switches on surfaces that are further removed from the current experimental state of the art are also performed and can give valuable insight as well as clues on which direction to turn [10,11]. An example of the latter is the computational study by Li et al. on the switching of hydrogen tautomerisation switches on several transition metal surfaces [10]. This family of switches shows promise towards use in complex nano-circuits, but so far, examples have only been able to be studied under cryogenic conditions.

2.11. Electrochemistry

Electrochemical methods can provide insight into the switching of molecules on surfaces if the redox chemistry is known for both states of the molecular switch. The data obtained from electrochemical measurements, potential and current, do not give direct information on the (changes in) molecular structure, however, and therefore the obtained information is limited when knowledge on the redox chemistry of the compound is limited also. The application of electrode potential is more useful as the stimulus for a change in molecular conformation, i.e. redox switching, for example in the electrochemical switching of self-assembled monolayers of overcrowded alkenes [104] and diarylethene-modified indium tin oxide (ITO) electrodes (Fig. 8) [38], and for driving reversible motion of a mechanically interlocked molecule in a metal-organic framework [42].

3. Surfaces and interfaces

In this section, several classes of surfaces and interfaces will serve as focus points for the techniques most often used and most suitable for each, in a discussion of surmounted challenges and persisting limitations. It is worth reiterating that the various classes of molecular switches and motors have distinct properties (see Section 1.1), e.g., the difference in electronic and vibrational absorption between the states. Furthermore, they can have varying interactions with surfaces made from different materials. Azobenzene, for example, adsorbs to various (metal) surfaces differently, resulting in specific orientation with respect to the surface, reactions with the surface (e.g., reduction), and resistance to switching (*vide infra*). With that said, the range of useful techniques for monitoring of switching will still depend greatly on the surface that has been modified with the switch. Of course, if switching of a certain adsorbed molecule does not result in significant changes in, for example, electronic absorption, then UV–Vis absorption spectroscopy is not the technique of choice. In the end, there will always be an interplay of parameters from both the surface and the immobilised molecule that will determine the range of techniques that can be used.

3.1. (More or less) atomically flat surfaces

Atomically flat surfaces are often used as substrates for functionalisation with molecular switches due to their well-established and generally predictable surface properties. Amongst the wide variety of metals (and other materials) available, gold is often the substrate of choice due to its advantageous properties. As with other metals, it is conducting; its thermodynamically most stable geometry, Au(111), is readily obtained when preparing gold surfaces, which facilitates fabrication; and most importantly, its reactivity with certain functional groups, e.g., thiols, means it is straightforward to form gold-adsorbate bonds in many cases (i.e. chemisorption).

Another strong interaction of gold is with aromatic units, which

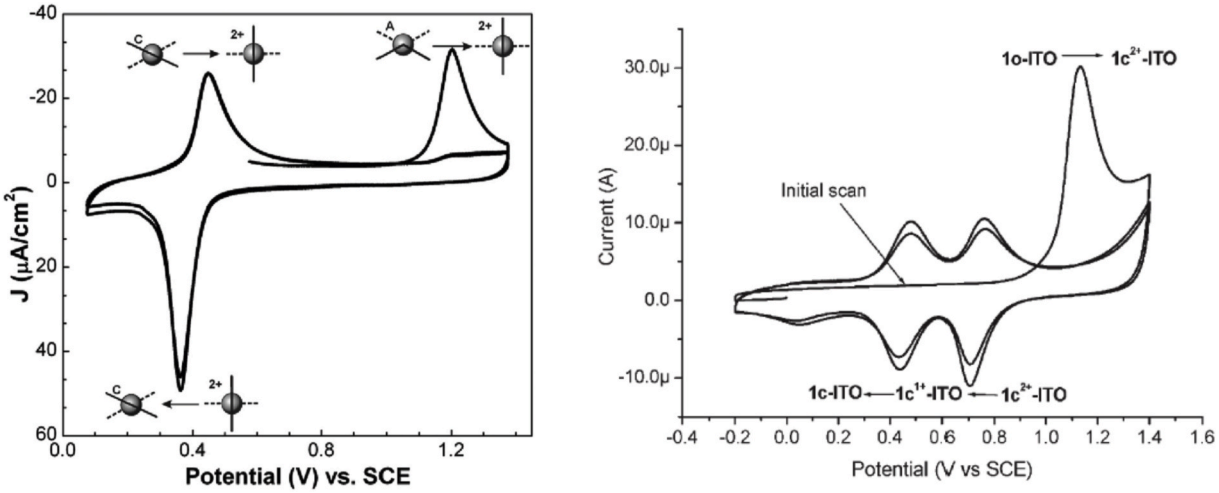

Fig. 8. Electrochemical switching of (left) self-assembled monolayers of an overcrowded alkene (dimethyl-bisthiaxanthylidene) on Au, adapted in part from Ivashenko et al. [104], with permission from the American Chemical Society, and (right) dithienylethene immobilised on activated indium tin oxide (ITO), adapted in part from Areephong et al. [38], with permission from The Royal Society of Chemistry.

Rusch et al. take advantage of in their work on the self-assembly of an azobenzene-functionalised platform (**azobenzene-TATA**) onto gold in such a way that the orientation of the switch is lateral (altitudinal) to the surface [41]. Characterisation of the azobenzene-functionalised gold surface by X-ray photo-electron spectroscopy (XPS) confirmed the presence of two different types of nitrogen atoms, as expected, since the nitrogen atoms in the azobenzene are in a higher oxidation state than those in the "feet" in contact with the gold surface. Angle-dependent NEXAFS measurements confirmed conclusions reached on the basis of STM data regarding the orientation of azobenzene on the surface, which contrasts clearly with vertically aligned azobenzenes [40]. Changes in the structure of **azobenzene-TATA** during irradiation were monitored by UV–Vis absorption spectroscopy (in transmission mode on Au(111) thin films), and NEXAFS spectra were recorded before and after each irradiation, with both techniques demonstrating photochemical *E-Z* isomerisation (Fig. 9). Notably, STM measurements did not show the expected differences between irradiated and non-irradiated samples regarding inter- and intramolecular distances, which shows that the technique could not be relied on for determining whether switching on gold had occurred in this case.

Another example of the potential that X-ray spectroscopies provide in research into the conformations of molecules on a surface is given by Nickel et al. in their study on the photochemical switching of a spirooxazine on atomically flat Au(111) [105]. Changes in the K-edge X-ray absorption spectrum of nitrogen (only present in the adsorbed molecules), assigned with the aid of DFT modelling, indicate switching of the spirooxazine from its closed to its open form upon UV irradiation. Since damage by the X-ray irradiation precluded kinetic analysis, differential UV–Vis reflectance spectroscopy was used for the observation of the small changes in absorption during irradiation (Fig. 9). With this combination of techniques, at room temperature thermal reversion back to the spirooxazine closed form after photochemical ring-opening was found to compete with desorption from the surface, whereas ring-closing could be induced photochemically by excitation with visible (red) light at 130 K.

A combination of HREELS and STM by Mielke et al. established that an imine analogue of azobenzene substituted with four *tert*-butyl groups, (*E*)-3,5-di-*tert*-butyl-*N*-(3,5-di-*tert*-butylbenzylidene)aniline (**TBI**), has the opposite relative thermodynamic stability of its *trans*- and *cis*-isomers when deposited onto a gold Au(111) surface [106]. Deposition onto gold from solution, with a *trans* majority, resulted in the self-assembly of the molecules with a likewise majority in the *trans* conformation. Heating of the **TBI**-Au(111) sample for 2 min, followed by cooling to 100 K again for the recording of HREEL spectra (Fig. 9), resulted in double bond isomerisation to the *cis* state, which turns out to be the stable isomer on Au(111).

A downside to the atomically flat substrates is the lack of surface enhancement of Raman scattering – for which roughened surfaces are needed – which will be discussed in the next section.

3.2. Nanoparticles and roughened surfaces

As evident from their name, roughened surfaces have a larger surface area than their "smooth" counterparts, and hence a higher surface density of adsorbates can be achieved. However, the properties (e.g., orientations) are less well-defined. A major advantage of roughened surfaces, in regards to available spectroscopic tools, is the possibility for surface enhancement of Raman scattering by interaction of light with the plasmon resonance of certain materials, e.g., gold, silver, and copper, as is done with surface- and tip-enhanced Raman scattering (SERS and TERS) spectroscopy [34,62,64]. SERS spectroscopy is particularly useful for studying molecules immobilised on nanoparticles, whose behaviour is similar to planar roughened surfaces but possess an important distinct aspect that determines physicochemical properties, namely, the dependence of the electronic absorption and surface plasmon resonance on the microscopic structure of the nanoparticles [107]. Again, often the element of choice for fabricating nanoparticles is gold, for the same reason stated above of readily formed Au-adsorbate bonds, and also to the convenient surface plasmon energy of gold allowing the use of near-IR lasers.

The immobilisation of photoswitches on nanoparticles for use in functional materials has received considerable attention in recent years, not least in the work of the Klajn group discussed here. Nanoparticles have a considerably higher surface-to-volume ratio than planar substrates, but the chemical behaviour of an immobilised switch is still that of one on a surface. Advantageously, the size of nanoparticles is such that they themselves often only have a modest effect on optical properties, and therefore spectroscopic methods typically employed in solution studies, e.g., UV–Vis absorption spectroscopy (Fig. 10), can be used to probe structural changes of the molecular switch.

Nanoparticles proved to be a convenient substrate to use to study the behaviour of surface-bound molecular switches in a mixed monolayer environment with a non-photo-switchable co-adsorbate [108]. Under such conditions, a question arises as to whether the switches are influenced only by the bulk solution in which the modified particles are suspended, or whether they should be considered being in a local

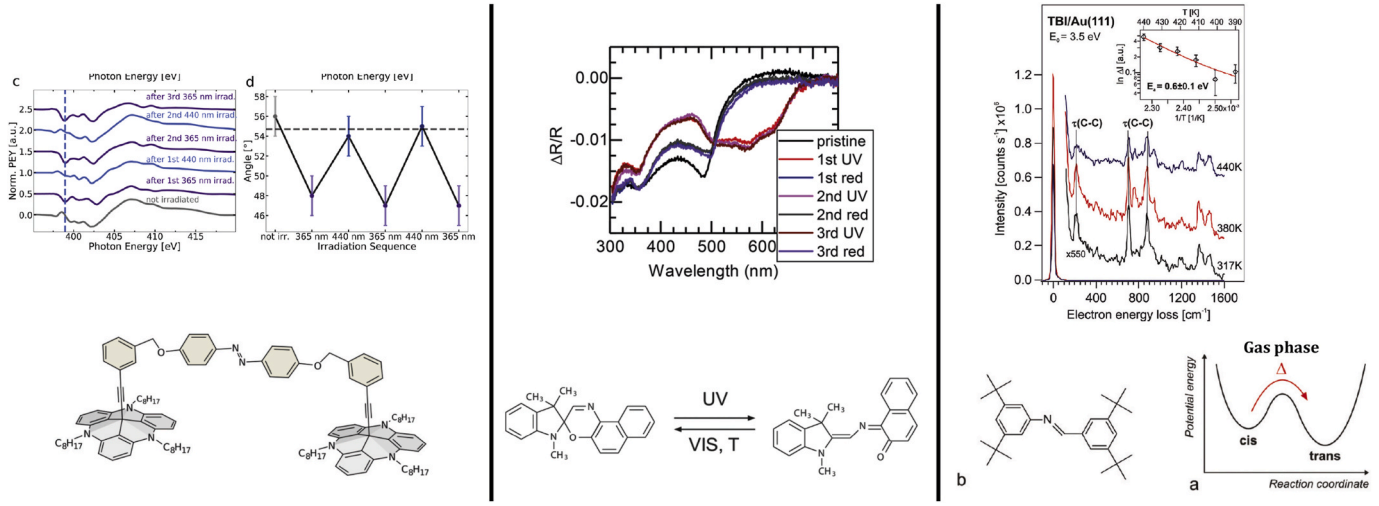

Fig. 9. (left) NEXAFS spectra of photochemical switching of **azobenzene-TATA** on Au(111) by Rusch et al. [41], (middle) differential UV–Vis reflectance spectra of photochemical switching of spirooxazine on Au(111) by Nickel et al. [105], and (right) HREEL spectra of TBI on Au(111) heated to various temperatures by Mielke et al. [106] Adapted in part from Rusch et al. [41], Nickel et al. [105], and Mielke et al. [106], with permission from the American Chemical Society.

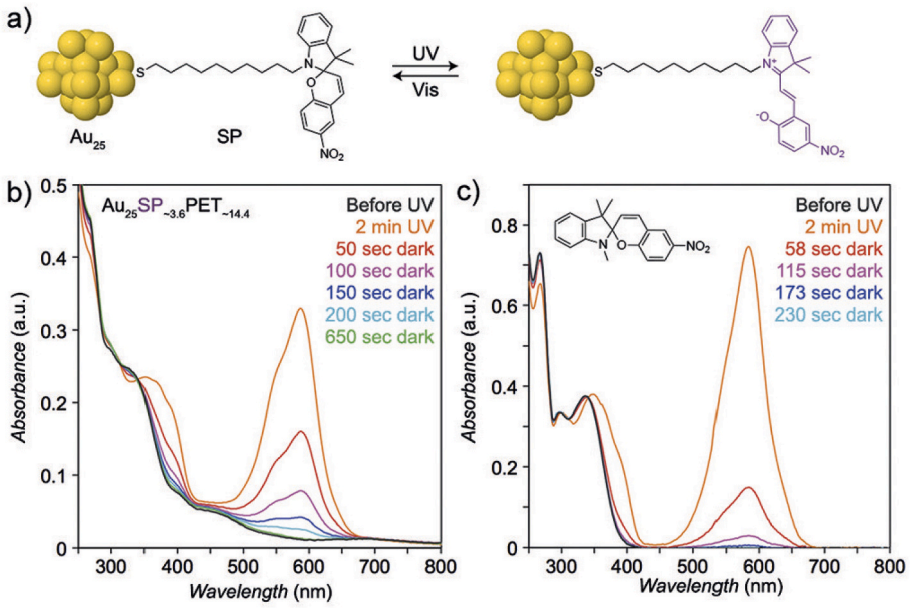

Fig. 10. a) Schematic representation of the reversible photochemical ring-opening and -closing of an alkylthiol-substituted nitrospiropyran immobilised on Au_{25} nanoclusters, b) corresponding UV–Vis spectra of immobilised nitrospiropyran on Au25 in THF before (black), after UV irradiation (orange), and after subsequent storing in the dark (red-green), and c) comparison with non-immobilised nitrospiropyran in THF before (black), after UV irradiation (orange), and after subsequent storing in the dark (red-blue) showing a higher rate of thermal ring-closing. Adapted in part from Udayabhaskararao et al. [92], with permission from WILEY-VCH Verlag GmbH & Co. KGaA, Weinheim. (For interpretation of the references to colour in this figure legend, the reader is referred to the Web version of this article.)

'solvent' environment created by the surrounding co-adsorbate as well as other molecules of the molecular switch and the double layer. Indeed, Klajn et al. found, using mixed monolayers of azobenzene whose *cis*- and *trans*-isomers are easily distinguished by UV–Vis absorption spectroscopy, that the local surface environment is of greater importance than the bulk solvent properties in regards to the photochemical behaviour of the immobilised switches, which allows for further tuning of the properties of the functionalised nanoparticles by introducing a co-adsorbate. In particles coated with mixed SAMs of azobenzene and alkylammonium bromide molecules, the difference in polarity between the *cis*- and *trans*-isomers enables changes in the overall hydrophobicity of the nanoparticles in water measured by the contact angle [108]. In another report, Klajn et al. characterised spiropyran-functionalised gold nanoclusters by ^{1}H NMR spectroscopy after fabrication [92], but did not use this technique to monitor photochemical switching. Besides the noted signal broadening due to the spiropyran being bound to the nanoparticles [109,110], another constraint is likely to have been the concentration of the photochemically generated merocyanine isomer being below the detection limit. Instead, the photochemically-induced ring-opening was observed using UV–Vis absorption and fluorescence spectroscopy (Fig. 10), while dynamic light scattering (DLS) enabled the detection of aggregates forming in toluene upon UV irradiation of the spiropyran-functionalised nanoclusters.

One feature of nanoparticles that should not be overlooked is the build-up of electric potential on the surface during continuous irradiation. This phenomenon has been investigated in the field of plasmonic photocatalysis [111], but can have consequences as well for any surface-confined molecule with a low enough redox potential. We go into more detail on the plasmon-driven chemistry on gold nanoparticles in Section 4.2.

3.3. Self-assembly and self-assembled monolayers

Self-assembly of molecules onto a substrate is driven by intermolecular interactions, which means that self-assembled monolayers (SAMs) are readily prepared by immersion of a (pre-treated) substrate in a solution of a compound with an appropriate anchoring group [112]. Monolayers can be formed on many different materials, but since the reactivity of the sulfur atom with gold is so high and the resulting gold-sulfur bond so strong, gold is an often-used substrate for the fabrication of self-assembled monolayers in combination with thiol- or disulfide-substituted compounds [113]. As discussed above, an obvious choice of characterisation method for these SAMs on (roughened) gold surfaces would be SERS or TERS.

An important parameter involved with the reactivity of SAMs is the amount of free volume available on the surface per molecule. For molecular switches, this plays a particularly large role when switching between isomers with large changes in conformation, e.g., *cis-trans* isomerisation. The minimum area required for isomerisation of azobenzenes is ca. $45 \overset{\circ}{A}^2$ molecule^{-1} [114–116], and Zharnikov et al. showed clearly the consequences of this critical limit with their study on dithiolane-substituted azobenzene SAMs on Au(111) [89]. SAMs prepared from a solution containing mainly *trans*-azobenzene did not exhibit photo-reactivity with respect to conversion to the *cis*-isomer, whereas those prepared from predominantly *cis*-azobenzene were able to undergo reversible *cis-trans* isomerisation. These results indicate a different manner of self-assembly, and therefore different available free volume per molecule, between the *trans*- and *cis*-isomer of azobenzene. The real time changes in isomerisation during irradiation were monitored using ellipsometry. The signal measured with this technique is the phase shift (Δ), which depends on factors such as packing density, film thickness, and film geometry [72]. The photo-isomerisation of azobenzene will result in a significant structural change, which in turn induces changes in the phase shift, thereby providing a simple means of monitoring switching between *cis*- and *trans*-isomer.

Kunfi et al. have reported the photochemical switching of azobenzene immobilised on a quartz substrate functionalised by polydopamine layers supporting gold particles (Fig. 11) [117]. Despite the inherent electronic absorption by the gold nanoparticles, the thin films allowed for characterisation of switching by UV–Vis absorption spectroscopy in transmission mode. This method is similar to that used by Zheng et al. [39], with the main difference that in the latter case the functionalised substrate was a thin metal film as well (10 nm).

3.3.1. The sulfur–gold bond

The study of binding of self-assembled monolayers onto gold surfaces is a multi-faceted problem incorporating various theoretical and experimental approaches to characterise, amongst other things, the nature of the gold-sulfur interaction [118,119], the various binding modes [119,120], and the condition-dependent formation of monolayers (e.g., pH, electric field, temperature) [121]. Computational studies focused on the gold-sulfur bond have noted that the strong

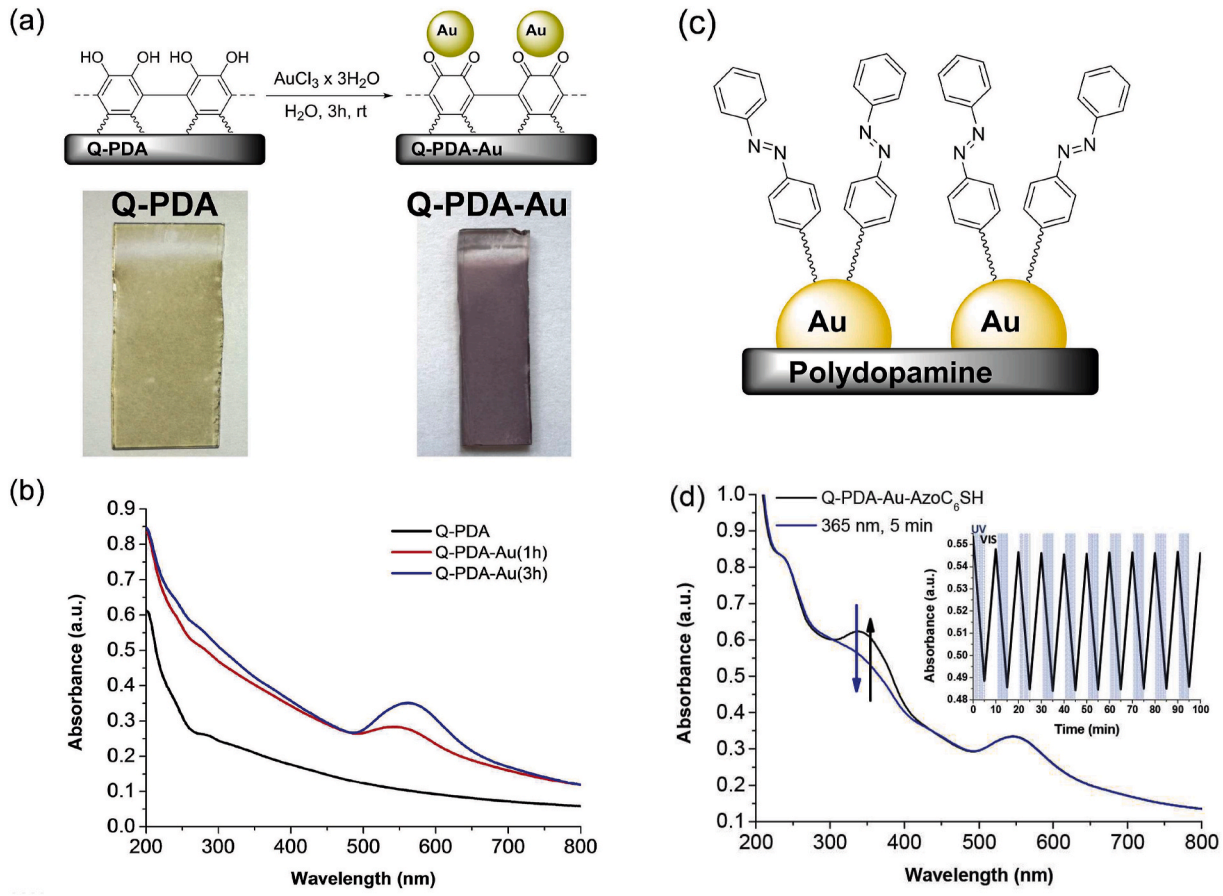

Fig. 11. (a) Schematic representation of the modification of a polydopamine-functionalised quartz slide (Q-PDA) with Au nanoparticles (Q-PDA-Au), and pictures of the corresponding changes in colour and (b) in solid-state UV–Vis spectra before (black), and after immersion of Q-PDA in an aqueous solution of $AuCl_3 \cdot x3H_2O$ for 1 h (red) and 3 h (blue), (c) Schematic representation of azobenzene self-assembled on Q-PDA-Au, and (d) solid-state UV–Vis spectra of Q-PDA-Au modified with an alkylthiol-substituted azobenzene before (black) and after irradiation at 365 nm (blue). Adapted in part from Kunfi et al. [117], with permission from WILEY-VCH Verlag GmbH & Co. KGaA, Weinheim. (For interpretation of the references to colour in this figure legend, the reader is referred to the Web version of this article.)

interaction between the gold and sulfur atoms results in a weakening of the gold-gold bonds around the site of adsorption and, consequently, a decrease of the barrier for surface diffusion of the "complex" formed by the adsorbate and the gold atom [122]. A notable conclusion drawn by Guesmi et al. is that for short-chain alkanethiols the mobility of adsorbate-Au complexes is higher than for longer-chain analogues due to weaker intermolecular interactions between the chains [119]. SAMs of molecular switches that are attached to gold with long alkyl chains, e.g., by Ivashenko et al. using spiropyrans [55], therefore should be relatively static [54].

Simple thiols such as thiophenol and methanethiol have often been used as model compounds for studying the binding between sulfur and gold. Rajaraman et al. performed a DFT study using a periodic approach to describe the Au(111) surface and concluded that the adsorbed species can be described as a thiyl radical ($RS^{\bullet}$) bound to gold [120]. The rate of self-assembly onto surfaces such as gold is dependent on pH. For thiophenol self-assembly, Tripathi et al. showed that, at low pH, the rate of formation is limited by physisorption (i.e. electrostatic interaction between thiophenol and gold), whereas at high pH the rate-limiting step is chemisorption (i.e. bond formation between the sulfur and gold) because of the majority of the molecules being in the deprotonated thiophenolate state [121].

Since gold has a convenient surface plasmon energy (of ca. 600–1000 nm) [62], an obvious choice of technique for investigating the (change in) molecular structure of self-assembled monolayers on (roughened) gold is surface-enhanced Raman spectroscopy when using a laser with a resonant wavelength (e.g., 785 nm) [123–125]. An alternative approach called *directional Raman scattering* was recently reported by Smith et al. which does not rely on surface enhancement, and therefore enables recording of Raman spectra of self-assembled monolayers on *non-roughened* gold surfaces [126,127]. Computational investigations using periodicity to simulate the surface of gold with adsorbed thiol-capped molecules were performed by Zayak et al. and show quantitative agreement with experimental SERS spectra [101]. Alternative methods without the use of periodical calculations, but instead opting for gold clusters to simulate the gold surface, have been used by Tetsassi Feugmo and Liégeois [128], and Saikin et al. [129], to obtain accurate calculated vibrational spectra as well, due to the inclusion of multiple adsorption sites and coordination modes.

3.4. Single molecules

There are various approaches to prepare single-molecule junctions, for example, by dispersion of the molecule of interest onto a surface mixed in with a monolayer of molecules with lower conductivity, and by the techniques scanning tunneling microscopy break junction (STMBJ) and mechanically controlled break junction (MCBJ) [130]. The single-molecule devices are characterised using conductance (G_0) measurements [1]; the difference in conductance of the molecular junctions before and after application of a stimulus, e.g., light, mechanical stretching, and chemical additives, is interpreted as the occurrence of switching – provided that the measured increase or decrease in current is in agreement with that expected from the electronic properties of the different states of the switch [131–136].

STM break junctions of a pyridine-terminated spiropyran between two gold electrodes fabricated by Walkey et al. [135] using the so-called "tapping" or current–stretching approach [137,138] showed no indication of ring-opening to the merocyanine isomer upon increasing the distance between the two gold surfaces – the current *vs* distance traces exhibit a plateau until G_0 drops to zero – and the molecular junctions break from their contact points before sufficient strain can be applied to break the C–O bond and form the (longer) merocyanine isomer.

The explored possibility of making molecular junctions with both the closed and open (protonated) forms made use of the acid–base chemistry of spiropyrans [139] in combination with an alternative method to determine the conductance: the so-called "blinking" or "I(t)" method [140,141]. In this experiment, both the STM tip and the surface are kept at a fixed position, and an increase in current is detected when a single molecule bridges the gap between the two electrodes. An important feature of this "blinking" method is that it allows the measurement of current-voltage properties of a single-molecule junction due to its relatively long lifetime (ca. 0.5 s). The mean conductance values without and with acid present – derived from conductance histograms containing data collected from many samples – determined with both methods of fabricating STM break junctions, are in good agreement. The agreement indicates that single-molecule devices can indeed be formed with both the closed spiropyran isomer and the protonated merocyanine isomer.

Reports by Darwish et al. [132] and Roldan et al. [131] likewise show the use of changes in (the magnitude of) conductance to indicate switching of the molecules that form the single-molecule junctions, using spiropyran and – thanks to nitro-substitution – its photochemically generated neutral open form, and the photoswitch dimethyldihydropyrene (DHP), respectively. Importantly, these reports have not shown the (acid-base and photochemical) switching of a molecule while still attached to both electrodes – instead, the protonation–deprotonation and photochemical isomerisation happen in the bulk solution prior to formation of the single-molecule junctions.

Mechanical ring-opening of a single spiropyran molecule was reported by Walkey et al. [135] for an alkyne-instead of pyridine-terminated derivative in an STM break junction, by stretching of the molecule in the junction, leading to breakage of the C–O bond. A spike in the conductance observed at a certain relative electrode distance, after the plateau in the current–distance curve assigned to the closed form, was the indication of ring-opening to the merocyanine form; the higher conductance being explained by the increased conjugation in the open isomer.

Photochemical switching of a single molecule while it forms a junction, reported by Meng et al. [134], allows the reversible optical control of a single-molecule transistor, in which a linear trisbenzene-based molecule is functionalised with an azobenzene side group. Current measurements at low bias voltages show that the conductance increases upon UV irradiation, generating the *cis*-isomer, and decreases again upon irradiation with visible light, switching back to the *trans*-form.

It is of note that a conductance measurement does not give direct insight into the molecular changes of the single molecule in the junction upon switching – the technique instead is linked to the electronic properties of the molecule while part of a particular junction. Information on the molecular structure of a single molecule that undergoes switching is available by means of enhanced vibrational spectroscopies such as surface- and tip-enhanced Raman spectroscopy (SERS and TERS, respectively). While the potential is clear of these techniques to provide direct insight into the changes that occur in a single molecule during, e.g., photo-induced isomerisation, the measurements themselves are of significant influence on the molecule being studied (see Section 2.4.2 for more details) [70]. Nevertheless, TERS and single-molecule SERS are a promising tool for probing single-molecule reactions on surfaces [69].

3.5. Metal-organic and covalent organic frameworks

Metal-organic and covalent organic frameworks (MOFs and COFs) are distinct from the other systems discussed here due to the absence of a bulk material that creates a surface. Over the past years, MOFs and COFs have been shown to be excellent frameworks for creating functionalised materials [142]. Incorporation of photo-responsive switching units in metal- and covalent organic frameworks is an attractive approach to tuning the physical properties of these low-density structures using light [5].

In contrast to 2D materials and thin films, the 3D structures allow for relatively straightforward characterisation by a wide range of structural and spectroscopic techniques, but present a particular challenge in optical characterisation and especially when light is used to control properties at the same time. The high number density of chromophores present, when used as a structural element, means that the penetration depth for light, i.e. thickness where 1% transmission is reached, is of the order of 500 nm (assuming a molar absorptivity of $1 \times 10^4\,M^{-1}cm^{-1}$ and a concentration of 0.4 M) [31]. For microcrystalline material, 500 nm is a significant depth, and by irradiation at the edge of an absorption band, depths of up to 10 μm can even be reached (provided the photo-product does not increase overall absorbance at the excitation wavelength). Hence, photochromic response can be expected well beyond the surface layers (the first tens of nm). However, these depths make characterisation by standard spectroscopic techniques challenging, such as UV–Vis and FTIR absorption spectroscopy, especially when the material is not stable to solvent loss [30]. Near-infrared (NIR) light, where electronic absorption is negligible for most commonly used molecular switches, has advantages for characterisation by Raman spectroscopy (λ_{exc} > ca. 700 nm). It is of note that many materials have vibrational overtone absorption bands in these regions also with molar absorptivities that are significant enough to result in sample heating under the high local power densities used.

Since UV–Vis absorption spectroscopy is a key technique in characterising the state of photochromes, overcoming the limitation of optical penetration depth is essential. Heinke and co-workers, in a series of studies in recent years, have used so-called surface-mounted MOFs (SURMOFs) in which MOFs are constructed on an optically transparent surface as a thin layer - and can therefore be viewed as a nanoporous thin film (Fig. 12) [143,144,145]. An example of these surface-grown MOFs is called HKUST-1, consisting of trimesic acid, copper(II) acetate, and azobenzene as the photoswitchable unit. Characterisation of HKUST-1 by X-ray crystallography was still possible and could be used to establish its crystal structure before and after incorporation of azobenzene, and after photochemical switching with UV light [45]. The homogeneous distribution of the azobenzene molecules within HKUST-1, measured by Time-of-Flight Secondary Ion Mass Spectrometry (ToF-SIMS), indicates that the majority of the molecules are loaded in the pores of the MOF. The film was sufficiently thin to allow for monitoring of the photochemical switching during irradiation by both UV–Vis absorption spectroscopy and infrared reflection-absorption spectroscopy (IRRAS). A further advantage of this thin film approach is that it enabled the use of a quartz crystal microbalance (QCM) to determine switching of the incorporated azobenzene indirectly by measuring the uptake of butanediol, which is dependent on whether the azobenzene is in the less polar (*E*) or more polar (*Z*) form.

These studies demonstrate elegantly how effective thin films can be in overcoming two major challenges in studying MOFs. Firstly, the inner filter effect is avoided by keeping the optical path length within acceptable limits, which makes SURMOFs accessible to routine spectroscopic techniques. Secondly, since the net diffusion of gas molecules is relatively fast only over short distances, the response of the systems is improved by having relatively few layers, and the thin layers are perfectly suited to the quartz crystal microbalance.

Heinke et al. have concluded from their studies that the reversible uptake or adsorption of molecules in (existing) switchable azobenzene

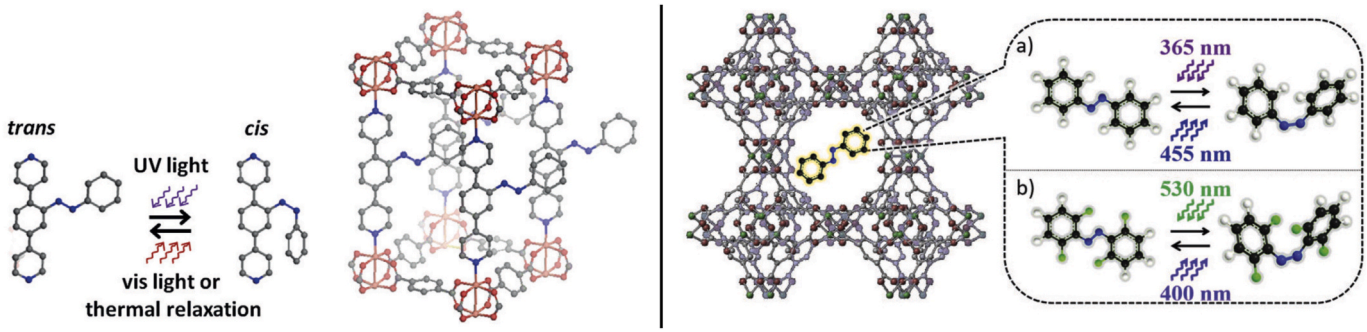

Fig. 12. Highly crystalline and oriented thin films of metal-organic frameworks on surfaces (SURMOFs) developed by Heinke et al. with the azobenzene photoswitch (left) incorporated into the framework [143] or (right) loaded into the pores of the MOF [45]. Reproduced from Wang et al. [143], with permission from 2015 WILEY-VCH Verlag GmbH & Co. KGaA, Weinheim, and adapted in part from Müller et al. [45], with permission from The Royal Society of Chemistry.

MOFs could be further improved by increasing the density of azobenzene moieties in the pores. Indeed, of several photo-switchable SURMOFs with various densities of azobenzene per pore volume, the highest density examples exhibited a larger switchable uptake ratio of probe molecules [146]. Chiral versions of azobenzene-functionalised SURMOFs, using D-camphoric acid as linker units (Fig. 13), lent themselves to characterisation by circular dichroism (CD) spectroscopy as well, in addition to the established techniques of UV–Vis and FTIR absorption spectroscopy [147]. Not unexpectedly, identical CD spectra were found for the *trans* and *cis* states, since the chiral centers are separate from the azobenzene groups in the MOF structure. Notably, QCM loading experiments showed that, in the *trans*-azobenzene state before irradiation, the chiral SURMOF performs preferential uptake of the (*S*)-enantiomer of a chiral probe molecule, while after irradiation to generate the *cis*-azobenzene isomer, the SURMOF did not show a preference for either enantiomer.

When a SURMOF was placed between two electrical contacts, the photo/isomerisation of an incorporated spiropyran could also be (indirectly) measured by monitoring the current over time while applying a constant DC voltage [148]. Upon UV irradiation, generating the open merocyanine isomer, the conductance increased, and it decreased gradually again after removal of the light source to allow for thermal ring-closing back to the spiropyran isomer. In general, conductance measurements should not be used as characterisation of molecular switching due to the indirect method of observation, but the technique is indeed suitable for the characterisation of macroscopic properties of a system.

Thanks to the large free volume for movement for the pendant azobenzenes, the azobenzene-functionalised SURMOF discussed above [143] was found to be a useful model system to study the energy barrier

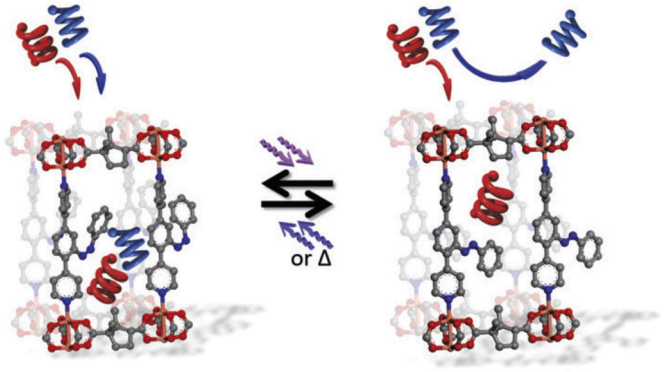

Fig. 13. Chiral SURMOF with D-camphoric acid linkers (horizontal) and azobenzene-containing pillars (vertical) shown in (left) *cis* and (right) *trans* state. Adapted in part from Kanj et al. [147], with permission from The Royal Society of Chemistry.

to thermal isomerisation of azobenzenes in different media by localised surface plasmon resonance (LSPR) spectroscopy [149].

With the aim of obtaining a higher level of control over the switching rates of photo-responsive MOFs, Shustova et al. prepared several frameworks with different linkers containing photoswitchable diarylethene or spiropyran units [150]. Photochemical switching, and thermal reversion in case of the spiropyran-functionalised MOFs, was confirmed by UV–Vis absorption spectroscopy in comparison with that of the photoswitches in solid state and solution. When the MOF contains linkers with a single spiropyran unit, solution-like photo-switching behaviour is obtained. Alternatively, when a different linker is used containing two photo-switching units, the spiropyrans show limited photo-isomerisation more similar to that in solid state, which is attributed to steric hindrance from proximity with each other in the framework.

UV–Vis–NIR reflectance spectroscopy was used by Chen et al. to study the reversible redox-controlled motion of a mechanically interlocked molecule (MIM) incorporated into a zirconium-based MOF [42], albeit indirectly by recording spectra before and after chemical oxidation and reduction of the MIM-MOF powder suspended in a solution containing the respective oxidant or reductant. A characteristic broad charge-transfer band at 1000 nm between two moieties of the interlocked rings, present in the neutral state, disappeared after chemical oxidation and reappeared after subsequent reduction, indicating relative circular motion of the two rings of the MIM. No dilution of the powder was necessary for the UV–Vis–NIR reflectance measurements, since the chromophore constitutes only a small percentage of the entire MIM-MOF system – it is inherently diluted in the framework to a sufficient degree. Deposition of the MIM-MOF onto a conductive fluorine-doped tin oxide (FTO) substrate allowed for characterisation of the redox chemistry by cyclic voltammetry, which showed a similar response as in solution. Unfortunately, though not commented on by the authors, *in situ* electrochemical switching monitored by UV–Vis–NIR reflectance spectroscopy was likely not possible due to experimental challenges.

The photochemical switching of metal-organic frameworks loaded with spirooxazine were studied by Ruschewitz et al. by means of UV–Vis and IR spectroscopy [47]. Spectra were recorded before and after UV irradiation of dilute solid samples prepared by mixing and grinding of the spirooxazine-MOF with KBr in a 1:12 ratio, followed by high-pressure compression into transparent pellets. This sample preparation allowed for acquisition of both UV–Vis and IR absorption spectra in transmission mode.

Raman spectroscopy offers an alternate approach to characterising photochemical switching in MOFs and COFs [30,35], making use of the change in molecular, and hence, vibrational structure. This technique was used by Danowski et al. [30] to demonstrate unidirectional rotary motion of a light-driven molecular motor incorporated as a linker unit in a metal-organic framework (Fig. 14).

The difficulty in this study was in identifying the functionality of the photochemically driven molecular motor. The challenge lay in the fact that the standard spectroscopic methods that would be used for such a system, such as UV–Vis and IR absorption spectroscopy, were hampered by the need to keep the MOFs in solution at all times, lest they lose their structure. Hence, diffuse reflectance methods were not applicable. In this regard, non-resonant Raman spectroscopy proved useful as the signal measured is not the difference in light intensity with and without sample (i.e. absorbance) but purely the Raman scattering intensity. Hence, the primary inner filter effect is avoided. However, the absorption of the solvent DMF and of the MOF at the applied laser wavelength (785 nm) was sufficient such that a key challenge during measurement was heating from the laser. This issue was solved by looking at the effect of the duration and intensity of excitation by the laser during the measurements on the rate of the thermal helix inversion (THI), i.e. the rate at which the system recovered after being irradiated with light. By lowering the power, the observed rate for THI eventually approached the value expected from molecular modelling and solution studies [30]. The results from this paper show that the amount of heat generated by a laser, even in an apparently non-absorbing sample, can be sufficient to affect relatively slow thermal processes. Furthermore, Danowski et al. show that the rate at which the motor is working is essentially identical to that observed in solution, which confirms that there is enough free space in the internal structure of the MOF for the functionality of the molecules to be retained. This observation has implications for the concept of molecular viscosity and viscosity in confined spaces [151].

In a general sense, the studies demonstrate that vibrational spectroscopy is exceptional for its use in extracting structural information from a sample, since a change in molecular structure directly results in a change in the shape of the Raman or IR spectrum. As a final note, a challenge that needs to be highlighted since the samples are aligned, is that there is a significant difference in the Raman spectra depending on the orientation of the single crystal of a MOF relative to the polarisation of the laser used.

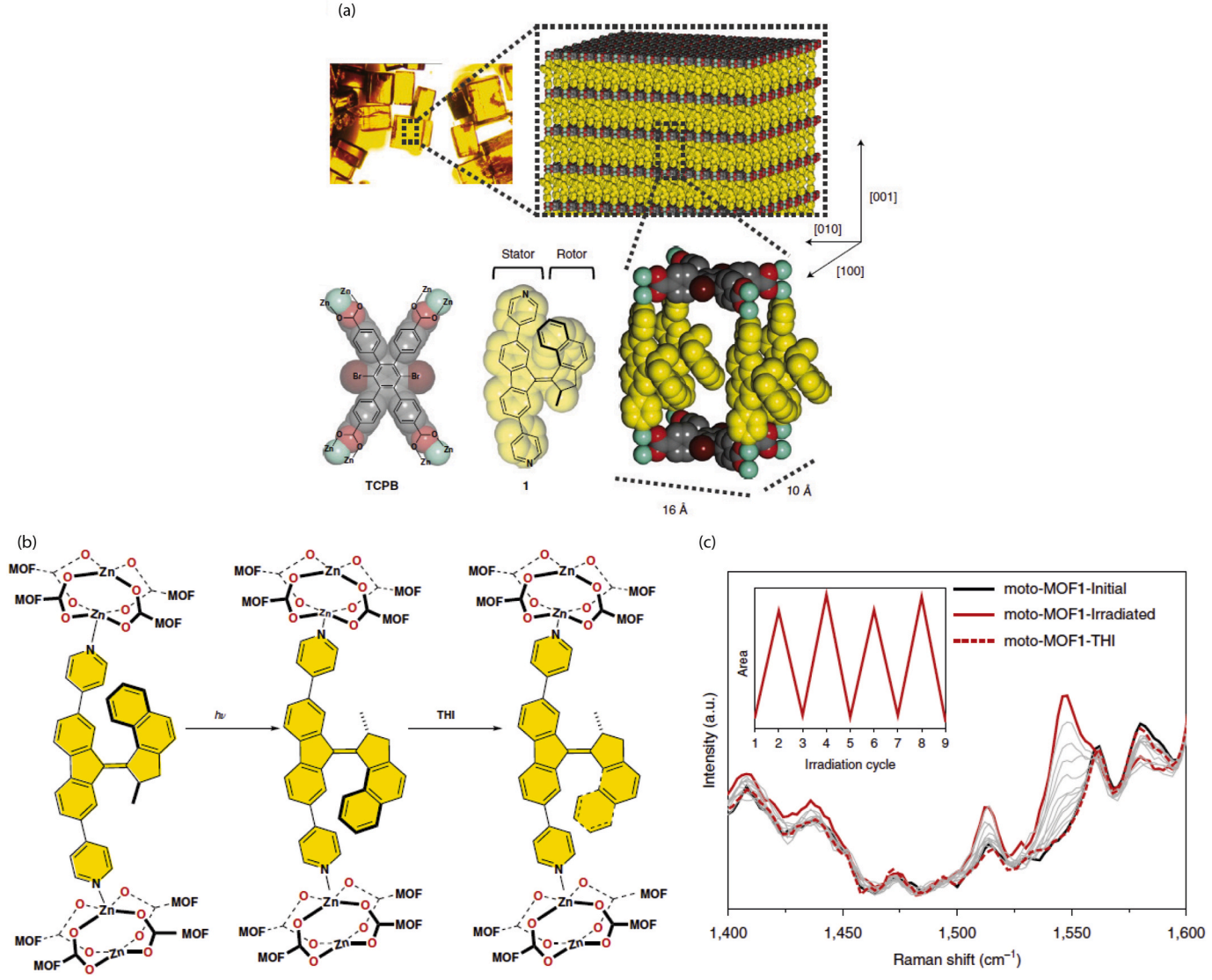

Fig. 14. (a) Microscopy image of crystals of a molecular motor incorporated into a MOF (moto-MOF**1**), and a schematic representation showing the packing in the crystal, the elementary cell, and the molecular structures of the linkers tetracarboxylic acid (**TCPB**) and the molecular motor **1**, (b) schematic representation of the structural changes of moto-MOF**1** after photochemical isomerisation and subsequent thermal helix inversion, and (c) changes in the Raman spectrum (λ_{exc} 785 nm) before (black) and after 395 nm irradiation (red, solid), and after subsequent thermal isomerisation at 20 °C (red, dashed). Adapted in part from Danowski et al. [30], with permission from Springer Nature. (For interpretation of the references to colour in this figure legend, the reader is referred to the Web version of this article.)

4. Case studies

4.1. Tip-enhanced Raman spectroscopy of hydrazone switches on metal surfaces

Hydrazone-based photochromic switches are a relatively recent addition to the category of molecular switches developed by the group of Aprahamian [152,153]. Their photochemical switching properties were first explored in detail in solution [154], and subsequently on several metal surfaces, namely gold, silver, and copper, by UV–Vis absorption and tip-enhanced Raman scattering (TERS) spectroscopy, as well as by DFT calculations [39]. The calculated Raman spectra of both *Z*- and *E*-isomers of an alkanethiol-substituted hydrazone photoswitch (**C6 HAT**) are in good agreement with the Raman spectra of both isomers collected in the solid state, and the solid-state Raman spectrum of the *Z*-isomer agrees well with the TERS spectrum of a monolayer of **C6 HAT** on gold before irradiation. These data exemplify the point that tip- or surface-enhanced Raman spectra should match solid-state non-resonant spectra where the molecular structure (conformations as well as bonding) in the SAM is essentially the same as in the solid state. A key challenge in such studies is sample degradation due to the highly focused lasers used, and although the TERS spectra did not indicate degradation due to laser heating, it was excluded with a positive control for thermal degradation using temperature-programmed desorption mass spectrometry (TPD-MS).

UV–Vis absorption spectroscopy of the monolayers was carried out on a 10 nm thick film of the metal (Au, Ag, or Cu) on quartz. Preparation of the sample in this way ensures that the metal substrate behaves chemically as a bulk metal but is still optically transparent, which means that spectra can be obtained in transmission (see also Section 2.2.1). For reference, UV–Vis spectra of the bare substrates were collected before preparation of the self-assembled monolayers of **C6 HAT** onto the metal. After *ex situ* irradiation with violet light (410 or 415 nm), the absorption maximum of the *Z*-form of the hydrazone SAM underwent a blue-shift which indicates *Z-E* isomerisation (Fig. 15). Heating the sample at 50 °C, which should induce back-isomerisation, results in an incomplete shift back to the original absorption spectrum, as well as a significant decrease of absorbance. These data indicate (incomplete) thermal *E-Z* isomerisation, and the authors ascribe the decrease of absorbance to degradation caused by heating of the sample. In regards to the sampling method, we note that the observed decrease in absorbance after heating could be due to a change in position of the sample as well.

All three metal surfaces used in this study were suitable for characterisation by TERS spectroscopy. An important note to make is that the substrate preparation for these measurements differ from that for the UV–Vis measurements discussed above, where a film of 10 nm thickness was prepared by physical vapor deposition of Au, Ag, or Cu onto quartz under high vacuum. For the TERS measurements, template-stripped Au and Ag substrates were prepared by thermal evaporation of a 200 nm film onto ultra-flat Si wafers, followed by attachment of a glass slide to the metal surface by UV-curable glue, and subsequent stripping of the Si wafer before use [12]. The Cu substrates were prepared by evaporation of a 5 nm thick layer of Cu onto the surface of freshly template-stripped Ag substrates.

SAMs of **C6 HAT** on both gold and copper underwent switching to the *E*-isomer upon irradiation at 415 nm manifested in changes in their TERS spectra, although the exact shift in band position is different to that observed in the solid state (e.g., 1562 *vs* 1580 cm^{-1} and 1704 *vs* 1730 cm^{-1} for solid-state and TERS spectra, respectively, Fig. 16). After heating of the SAMs on gold, while partial thermal recovery of the initial *Z*-isomer was observed by reappearance of bands at 1430 and 1472 cm^{-1}, an explanation for the apparent absence of the characteristic band at 1506 cm^{-1} was complicated by the lower signal-to-noise ratio of the TERS spectrum.

It is important to know the temperature at the surface of the metal substrate since this has an influence on the photostationary state of **C6 HAT** SAMs that can be reached due to the possibility of thermal *E-Z* isomerisation. The temperature was measured by temperature-programmed desorption mass spectrometry (TPD-MS) during irradiation of a **C6 HAT** SAM on Au at 415 nm. The temperature reached up to 45 °C after 15 min. The temperature at the apex of the silver tip (the so-called hotspot) used for TERS spectroscopy is of interest for the same reason regarding the photostationary state as well as thermally induced desorption (which occurs at 190 °C for **C6 HAT** on Au). Since plasmon-induced heating increases with laser power, a low power (70 μW) was used for all TERS measurements, which corresponds to a temperature at the tip apex of around 30 °C [155].

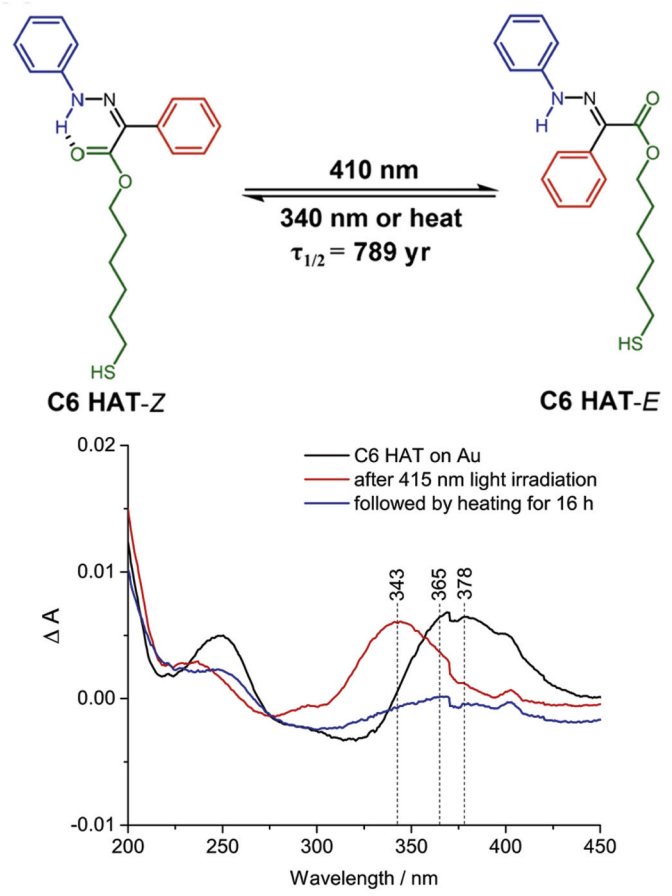

Fig. 15. (top) Thiol-substituted hydrazone photoswitch **C6 HAT** and its photochemical *Z-E* isomerisation, and (bottom) UV–Vis absorption spectra of a **C6 HAT** SAM on Au before (black) and after irradiation at 415 nm (red), and after heating at 50 °C in the dark for 16 h (blue). Adapted in part from Zheng et al. [39], with permission from the American Chemical Society. (For interpretation of the references to colour in this figure legend, the reader is referred to the Web version of this article.)

These temperature measurements show that both during 415 nm irradiation and during acquisition of TERS spectra no desorption is expected, and indeed none is observed after irradiation. However, the temperature of 45 °C reached under irradiation at 415 nm is close to that of 50 °C applied by the authors to induce thermal switching back to the *Z*-isomer, which means that the temperature could have a significant influence on the PSS_{415nm} of **C6 HAT** SAMs on gold.

In contrast to the functionalised gold and copper surfaces, the photoswitchable hydrazone molecules on silver were unaffected by irradiation at 415 nm. Only when using a shorter wavelength light source (280 nm) did the TERS spectra also indeed show the same characteristic bands of the *E*-isomer at 1580 and 1730 cm^{-1}. A key point to be derived from this work is that the observed lack of switching on silver at 415 nm was not due to chemical degradation or reaction of the adsorbed molecules with

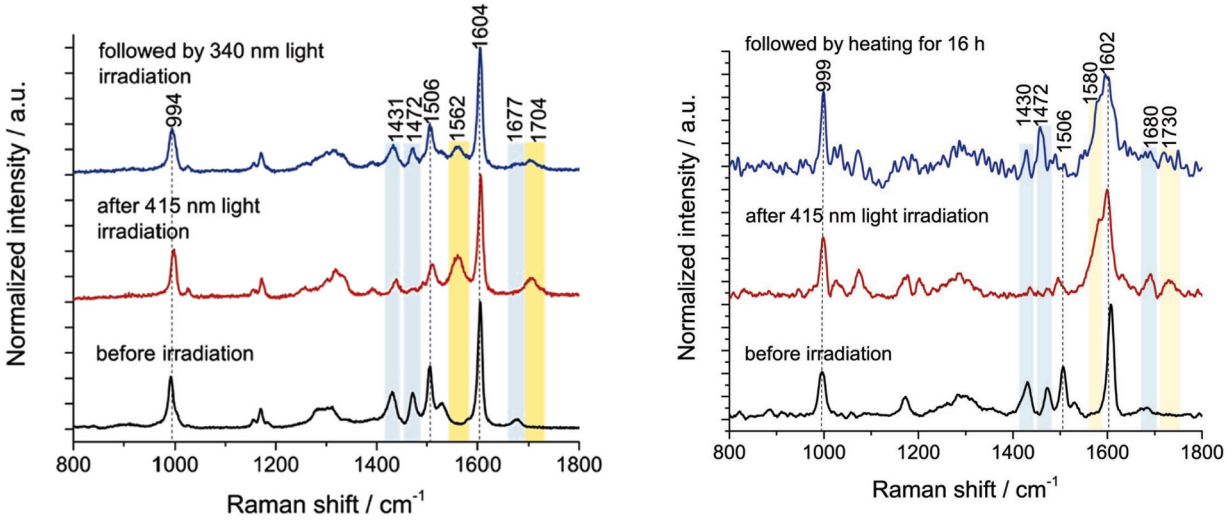

Fig. 16. (left) Solid-state spectra of **C6 HAT** before (black) and after irradiation at 415 nm (red) and subsequently at 340 nm (blue). (right) TERS spectra of **C6 HAT** on Au before (black) and after irradiation at 415 nm (red), and after subsequent heating at 50 °C for 16 h (blue). Blue bars indicate Raman bands of *Z*-isomer; yellow bars of *E*-isomer. Adapted in part from Zheng et al. [39], with permission from the American Chemical Society. (For interpretation of the references to colour in this figure legend, the reader is referred to the Web version of this article.)

silver, but rather due to the optical properties of the surface and the respective surface energy levels of the various metals.

Since both tip-enhanced Raman scattering spectroscopy and UV–Vis absorption spectroscopy were used by Zheng et al. to study switching of **C6 HAT** SAMs on metal surfaces, a clear comparison can be made between the two techniques. The advantage of (surface-/tip-enhanced) Raman spectroscopy over absorption spectroscopy of thin films shown nicely here is that Raman spectroscopy does not require a reference signal whereas absorption spectroscopy relies on the difference in signal intensities between a sample and a reference in order to obtain spectra in transmittance. The signal intensity of the reference is difficult to hold constant, especially when dealing with absorbances of <0.01, and makes this technique experimentally challenging.

A benefit of TERS spectroscopy is that the STM tip can be moved around and can therefore be used to record a two-dimensional TERS map in order to obtain statistical information regarding the photochemical conversion of **C6 HAT** SAMs on a larger part of the gold surface, in this case 1 × 1 μm^2. The averaged TERS spectrum of this map indicated the presence of 82% of the molecules in the *E*-form, calculated from the ratio of Gaussian functions fitted to the bands at 1680 (*Z*) and 1730 (*E*) cm^{-1}. This is in agreement with the calculated probability of finding another (stronger) characteristic band of the *E*-isomer, at 1580 cm^{-1}, in the TERS map.

4.2. Plasmon-driven chemistry on gold nanospheres

The various plasmon-driven chemical processes that can occur on gold nanoparticles were studied by Van Duyne et al. using SERS spectroscopy of *trans*-1,2-bis(4-pyridyl)ethylene (**BPE**) adsorbed onto gold nanosphere oligomers [65]. In particular, the effect of excitation into the plasmon band, in a region of the EM spectrum where the photoactive molecules on the particles do not have electronic absorption, was probed for its effect on the chemistry and structure of adsorbed molecules. Under these conditions, adsorption site hopping, photochemical reduction, and *trans-cis* isomerisation of **BPE** all occur (Fig. 17), which explains the observed stochastic behaviour of the SERS spectra during the measurement: several Raman bands appeared only in some spectra (Fig. 18).

The observation of these so-called fluctuations during pump-probe SERS measurements, i.e. recording of a SERS spectrum (probe at λ_{exc} 785 nm) after irradiation (pump at λ_{exc} 532 nm), is a good example of the

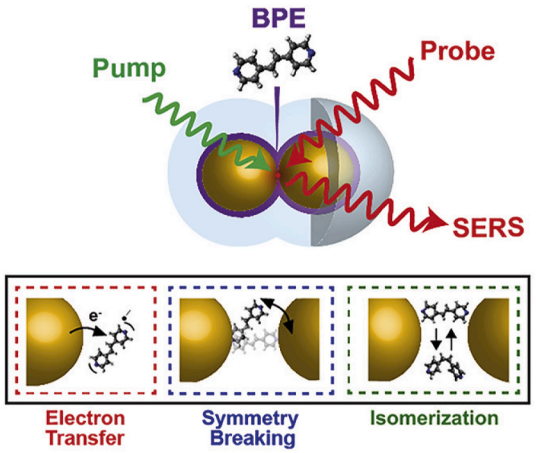

Fig. 17. Plasmon-driven chemical processes of **BPE** on gold nanoparticles. Reproduced from Sprague-Klein et al. [65], with permission from the American Chemical Society. (For interpretation of the references to colour in this figure legend, the reader is referred to the Web version of this article.)

care that should be taken with spectroscopic measurements of photochemically active compounds on surfaces. Notably, the averaged SERS spectrum resembles closely that of the initial spectrum of neutral **BPE** before irradiation, which indicates that only a small percentage of molecules on the surface undergo these plasmon-driven chemical transformations that are the cause of the transient Raman bands.

Regarding the assignment of the transient species, the Raman band at 1555 cm^{-1}, there is good agreement between the resonance Raman spectrum of the **BPE** radical anion in solution and the species produced on the nanospheres through plasmon-driven electron transfer. The variation in peak intensities of this band at 1555 cm^{-1} are thought to be due to differences in molecule-surface interactions, such as due to a changing local potential [156] or the excitation of dark plasmon modes [157]. The stochastic behaviour is attributed to the decay (i.e. oxidation back to neutral state, and degradation) and diffusion away from the high surface-enhancement sites, combined with the fact that the **BPE** radical anion formed is resonant with the excitation wavelength of 785 nm (while the neutral state is not), providing an additional mechanism of enhancement (resonance and surface plasmon enhancement).

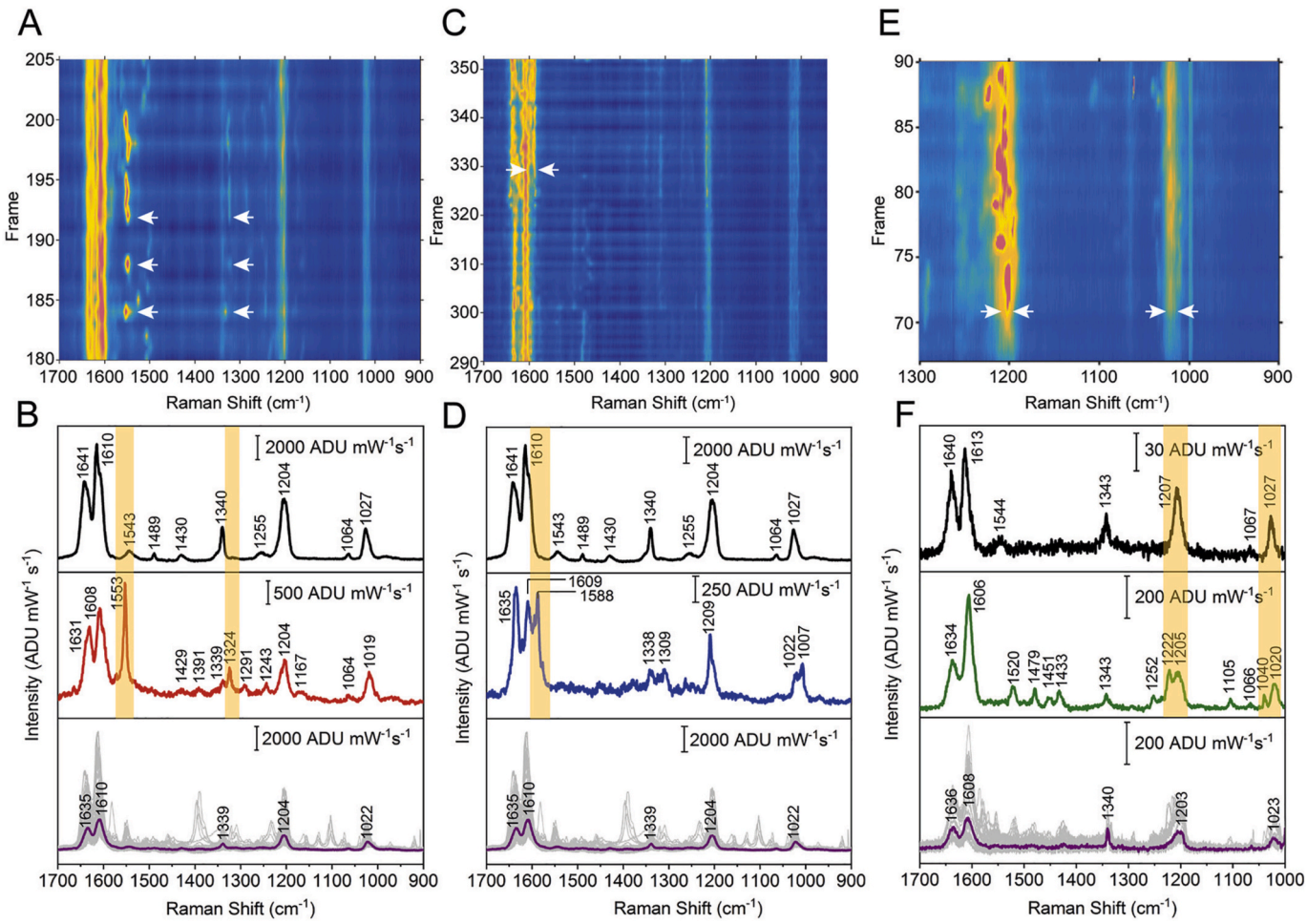

Fig. 18. SERS spectra recorded during pump-probe measurements of **BPE** on gold nanosphere oligomers by Sprague-Klein et al. depicting transient species with bands observed at (A&B) 1553 cm^{-1} assigned to the **BPE** radical anion, (C&D) 1588 cm^{-1} and 1209 cm^{-1} assigned to a change between face and vertex binding state of **BPE** to the gold cluster, and (E&F) 1222 cm^{-1} assigned to *trans-cis* isomerisation of **BPE**. Reproduced from Sprague-Klein et al. [65], with permission from the American Chemical Society. (For interpretation of the references to colour in this figure legend, the reader is referred to the Web version of this article.)

The authors explore the use of an insulating silica coating on the gold nanospheres to protect against build-up of charge during continuous irradiation [111]. In this case, it would be expected that no (or, at the least, less) reduction of **BPE** occurs during SERS measurements and, indeed, there is a difference in extent of generation of the **BPE** radical anion between silica-coated and bare gold nanospheres. 84% (2989 out of 3612) of the transient spectral features in the time-dependent SERS measurements were accounted for with known species, and the remaining signals were ascribed to possible **BPE** decomposition species and the excitation of near-field plasmonic field gradients [158,159].

4.3. Challenges in Characterising Switching on a surface

Unproductive and undesired reactions of adsorbed molecules can occur upon functionalisation of a surface, and can arguably make observations more difficult during measurements attempting to gather information on molecular switching on the surface. The non-zero chance of excitation at wavelengths where adsorbed molecules do not show electronic absorption (judged from a recorded absorption spectrum), e.g., in the near-IR, is due to two-photon absorption, which happens with low probability, but is still observed at interfaces [75]. For instance, the two-photon photochemical switching, with near-IR light, of spiropyrans to a merocyanine form is well-documented [160–162], however, the power densities needed are typically generated only with pulsed laser sources. Less expectedly, therefore, continuous wave lasers used for Raman spectroscopy can induce two-photon excitation when sufficiently focused, for example with a 50- or 100-times microscope objective focusing 100 mW onto a spot of as little as <3 μm diameter. This was exemplified in the photochromic switching of a spiropyran self-assembled monolayer on gold during the recording of surface-enhanced Raman spectra with near-IR light [55].

Combining techniques to study modified surfaces is advantageous in excluding experimentally-induced effects and artefacts, i.e. non-innocence of the technique. In regard to surfaces modified with (sub-) monolayers of compounds, in the range of techniques that can be applied generally, X-ray photo-electron spectroscopy (XPS) stands out as being highly versatile. However, caveats need to be made in such an approach, for example, in the study of SERS active (also called "roughened") surfaces. Ivashenko et al. showed that self-assembled monolayers of spiropyrans on electrochemically roughened gold surfaces undergo reduction of the nitro group during XPS measurements but not during SERS spectroscopic measurements (Fig. 19) [36]. Exposure time-dependent photoemission spectra of a model compound (a disulfide-terminated *para*-nitrophenyl alkyl ester) confirmed that the residual hydrogen present in the atmosphere of the XPS instrument was responsible and that, since reduction of the nitro group was not observed on relatively atomically flat gold surfaces, the roughened bulk gold substrate was responsible for an elevated activity towards reduction. A similar influence of the conditions in an XPS sample chamber was reported by Barriet et al. when the partial dehydration of

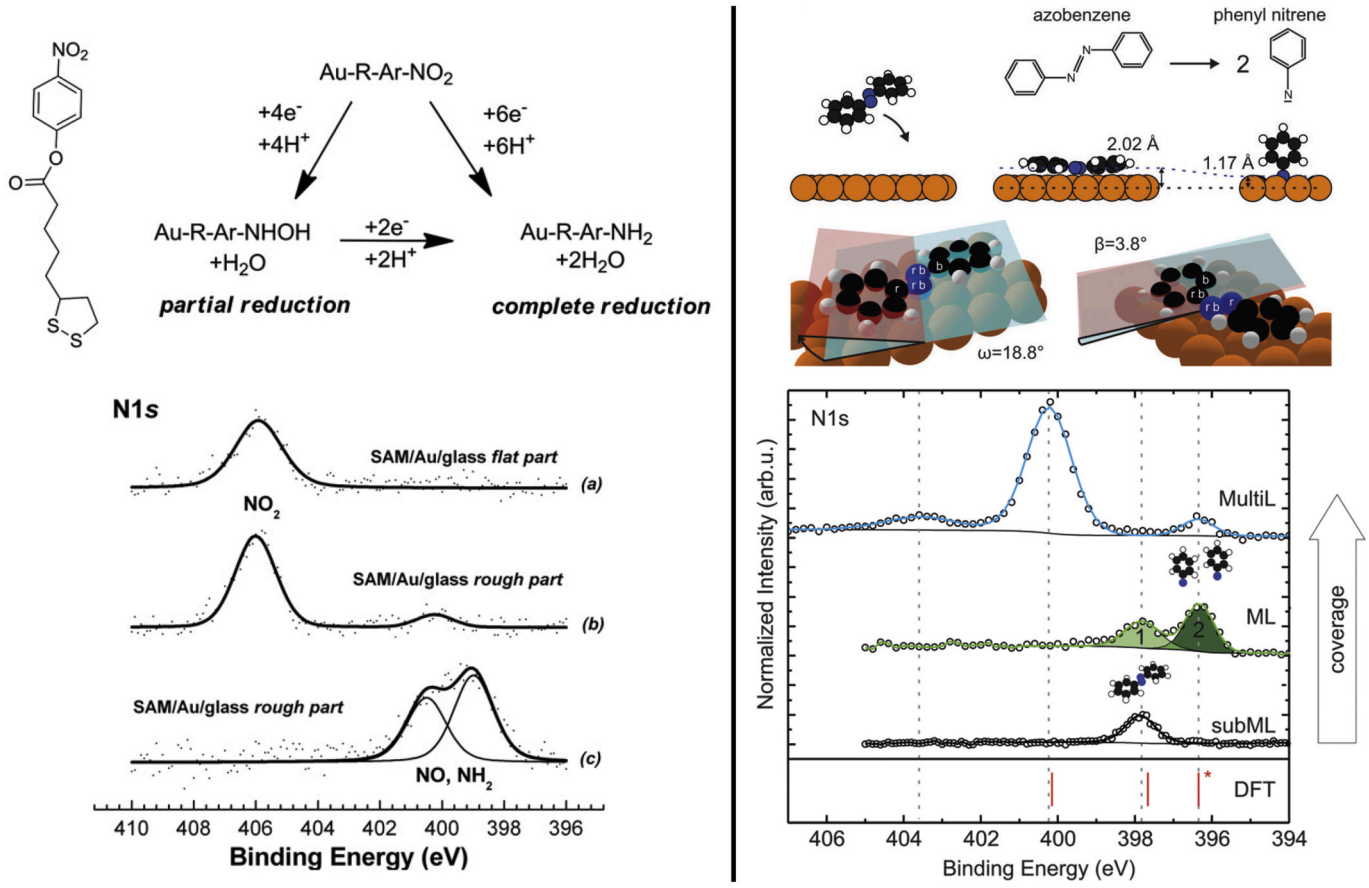

Fig. 19. (left, top) Possible mechanism for reduction of a disulfide-terminated *para*-nitrophenyl alkyl ester. (left, bottom) The N 1s photo-emission spectra of its SAM on a smooth (a) and a roughened (b) Au/Cr/glass substrate and after exposure to electrons (c) with a kinetic energy of 0.5 eV for 30 min in an XPS instrument. Adapted in part from Ivashenko et al. [36], with permission from Elsevier B.V. (right, top) Schematic depiction of dissociation of azobenzene to phenyl nitrene on Cu (111), and a 3D structural model of azobenzene in the adsorption geometry that it adopts in the sub-monolayer regime. (right, bottom) N 1s photo-emission spectra of a multilayer (MultiL), monolayer (ML), and sub-monolayer (subML) of azobenzene on Cu(111), with free (gas-phase) azobenzene at 400.1 eV, azobenzene adsorbed onto Cu(111) at 397.6 eV, and phenyl nitrene on Cu(111) at 396.3 eV. Adapted in part from Willenbockel et al. [164], with permission from The Royal Society of Chemistry.

4-mercaptophenylboronic acid SAMs in ultra-high vacuum resulted in boronic anhydride species on the gold surface [163].

Soubatch et al. reported the tendency of azobenzene on Cu(111) to undergo N–N bond cleavage to yield phenyl nitrene (Fig. 19) [164]. The extent of dissociation depends on the surface coverage – a sufficiently high density of azobenzene molecules on Cu(111) leads to quantitative dissociation to form phenyl nitrene. In contrast, dissociation was not observed on Ag(111). This difference in behaviour of azobenzene was attributed to the stronger interaction between the photoswitch and the copper surface resulting in surface-bound phenyl nitrene being the most stable structure.

In a related study, Piantek et al. show the difference in binding and conformational structure of dimetacyanoazobenzene (**DMC**) on Au(111) and Cu(001) [165]. Molecules on Au(111) show only physisorption, with the electronic structure similar to that calculated for the free molecule, while **DMC** on Cu(001) shows a mix of physi- and chemisorbed molecules at 150 K and, after annealing at 250 K, adopts a fully chemisorbed state. Furthermore, the higher the density of the coverage of **DMC** on Cu(001), the more a butterfly-like bent shape is adopted, until finally N═N bond breaking occurs.

The examples discussed above highlight the non-innocence of various commonly used techniques and surfaces. The relative importance of undesired effects in the application of a technique depends on the specific surface under study also.

5. Conclusions

From this overview of characterisation of molecular switching on surfaces, summarised in Table 1, it has become clear that, no matter the technique of choice, there are limitations to the information that can reliably be obtained from the measurements, since experimental conditions and sample preparation always have an influence on the system under study. It is imperative to be aware of and understand the precise effects of the applied characterisation method, and its combination with other parameters such as the adsorbed/immobilised compound and the substrate that is functionalised. Hence, investigations into the more basic and fundamental phenomena are essential for researchers using those characterisation methods to understand their functionalised surfaces.

Ideally, the technique used to study a system does not interfere significantly with that system during a measurement. Therefore, in general, when one is looking for a suitable means for characterising their functionalised surface, it is essential to search the literature for reports using similar samples, to read in detail the experimental requirements and challenges, and then to decide whether to use the same approach or to try an alternative that shows more promise. In this light, the scientific community benefits from thorough and detailed investigations into the interplay between technique, substrate, compound, and experimental conditions, many of which have been discussed here.

Table 1
Overview of techniques discussed in this review and their common uses, strengths, and limitations.

Technique		Common Uses	Strengths	Limitations
Absorption	UV–Vis–NIR	Thin (metal) surfaces (ca. 10 nm); SAMs	Switching usually paired with chromism; various modes available (e.g., transmission, reflectance)	Concentration range; scatter
	IR	Atomically flat surfaces; SAMs;	No light-induced switching; various modes available (e.g., transmission, reflectance)	Heating; sample thickness limit for ATR mode
	X-ray	Atomically flat surfaces	Provides information on the probed atom (XANES/NEXAFS) as well as on the neighbouring atoms (EXAFS)	Damage to sample (e.g., ionisation); requires synchrotron facilities (unless sufficiently high concentration)
Emission	UV–Vis–NIR	Luminescent switches	Zero-background	Photodamage; requires high quantum yield; inner filter effect
	X-ray	Atomically flat surfaces	Alternative means of obtaining absorption spectrum *via* excitation spectrum	Damage to sample (e.g., ionisation); requires synchrotron facilities (unless sufficiently high concentration)
Raman	Normal	Thin films; COFs & MOFS; phonons	Reference signal not needed; generally applicable; polarisation-dependent	Requires high concentration; scatter; fluorescence
	Resonance	Polymers; SAMs	Enhancement inherent to analyte	Requires availability of desired laser wavelength; thermal damage
	SERS	Roughened surfaces; nanoparticles; single-molecule	Simple experimental setup (similar to normal Raman); enhancement due to surface (and mostly independent of analyte)	Sensitive to impurities: signal originates from few sites (“hot spots”); plasmon-driven reactivity; thermal damage
	TERS	Atomically flat surfaces; single-molecule	Simultaneous STM information; surface need not be rough	Irradiation *in situ* challenging; plasmon-driven reactivity
XPS		SAMs; roughened and atomically flat metal surfaces	Information on oxidation state and bonding interactions	Damage to sample (e.g., ionisation); requires vacuum; irradiation *in situ* challenging
HREELS		Atomically flat surfaces	Different selection rules	Requires ultra-high vacuum
LSPR & Ellipsometry		Thin films; nanoparticles	Information on surface properties	Indirect information on adsorbed molecules
Non-Linear Optics		Noble metals	Signal only comes from surface; increased spatial resolution	Requires advanced instrumentation
NMR		Nanoparticles; MOFs (solid-state NMR)	Provides clear information on molecular structure	Limited applicability
Computational Chemistry		Spectral interpretation (e.g., X-ray spectroscopies); mechanisms; design of new and improved molecular switches	Possibility to venture into more unknown territories	Molecular models of functionalised surfaces usually deviate significantly from experiments
Electrochemistry		Stimulus (redox switching)	Direct control over oxidation state	Does not provide direct information on molecular structure; requires prior knowledge of redox chemistry

Declaration of competing interest

The authors declare that they have no known competing financial interests or personal relationships that could have appeared to influence the work reported in this paper.

Acknowledgements

Andy S. Sardjan is gratefully acknowledged for discussions on various topics covered in this review. Financial support was provided by The Ministry of Education, Culture and Science of the Netherlands (Gravity Program 024.001.035 to J.D.S., and W.R.B.) and the University of Groningen (DRD).

References

[1] S.J. van der Molen, P. Liljeroth, Charge transport through molecular switches, J. Phys. Condens. Matter 22 (2010), 133001. https://iopscience.iop.org/article/10.1088/0953-8984/22/13/133001, 10.1088/0953-8984/22/13/133001.
[2] X. Huang, T. Li, Recent progress in the development of molecular-scale electronics based on photoswitchable molecules, J. Mater. Chem. C 8 (2020) 821–848. https://pubs.rsc.org/en/content/articlelanding/2020/tc/c9tc06054e, 10.1039/C9TC06054E.
[3] J.M. Abendroth, O.S. Bushuyev, P.S. Weiss, C.J. Barrett, Controlling motion at the nanoscale: rise of the molecular machines, ACS Nano 9 (2015) 7746–7768. https://pubs.acs.org/doi/10.1021/acsnano.5b03367, 10.1021/acsnano.5b03367.
[4] X. Yao, T. Li, J. Wang, X. Ma, H. Tian, Recent progress in photoswitchable supramolecular self-assembling systems, Adv. Opt. Mater. 4 (2016) 1322–1349, https://doi.org/10.1002/adom.201600281, wiley.com/10.1002/adom.201600281.
[5] W. Danowski, T. van Leeuwen, W.R. Browne, B.L. Feringa, Photoresponsive porous materials, Nanoscale Adv. 3 (2021) 24–40. https://pubs.rsc.org/en/content/articlelanding/2021/na/d0na00647e, 10.1039/D0NA00647E.
[6] B.L. Feringa, W.R. Browne (Eds.), Molecular Switches, Wiley-VCH, 2011.
[7] A. Staykov, J. Areephong, W.R. Browne, B.L. Feringa, K. Yoshizawa, Electrochemical and photochemical cyclization and cycloreversion of diarylethenes and diarylethene-capped sexithiophene wires, ACS Nano 5 (2011) 1165–1178. https://pubs.acs.org/doi/10.1021/nn102806z, 10.1021/nn102806z.
[8] A. Perrier, F. Maurel, D. Jacquemin, Single molecule multiphotochromism with diarylethenes, Acc. Chem. Res. 45 (2012) 1173–1182. https://pubs.acs.org/doi/10.1021/ar200214k, 10.1021/ar200214k.
[9] R. Russo, A. Fihey, B. Mennucci, D. Jacquemin, Theoretical quantification of the modified photoactivity of photochromes grafted on metallic nanoparticles, J. Phys. Chem. C 120 (2016) 21827–21836. https://pubs.acs.org/doi/10.1021/acs.jpcc.6b07776, 10.1021/acs.jpcc.6b07776.
[10] J. Li, S. Yang, J.-C. Ren, G. Su, S. Li, C.J. Butch, Z. Ding, W. Liu, Deep molecular orbital driven high-temperature hydrogen tautomerization switching, J. Phys. Chem. Lett. 10 (2019) 6755–6761. https://pubs.acs.org/doi/10.1021/acs.jpclett.9b02671, 10.1021/acs.jpclett.9b02671.
[11] L. Le Bras, C. Lemarchand, S. Aloïse, C. Adamo, N. Pineau, A. Perrier, Modeling photonastic materials: a first computational study, J. Chem. Theor. Comput. 16 (2020) 7017–7032. https://pubs.acs.org/doi/10.1021/acs.jctc.0c00762, 10.1021/acs.jctc.0c00762.
[12] E.A. Weiss, G.K. Kaufman, J.K. Kriebel, Z. Li, R. Schalek, G.M. Whitesides, Si/sio2-templated formation of ultraflat metal surfaces on glass, polymer, and solder supports: their use as substrates for self-assembled monolayers, Langmuir 23 (2007) 9686–9694. https://pubs.acs.org/doi/10.1021/la701919r, 10.1021/la701919r.
[13] A. Caragheorgheopol, V. Chechik, Mechanistic aspects of ligand exchange in au nanoparticles, Phys. Chem. Chem. Phys. 10 (2008) 5029–5041. https://pubs.rsc.org/en/content/articlelanding/2008/cp/b805551c, 10.1039/b805551c.
[14] M.J. Hostetler, A.C. Templeton, R.W. Murray, Dynamics of place-exchange reactions on monolayer-protected gold cluster molecules, Langmuir 15 (1999) 3782–3789. https://pubs.acs.org/doi/10.1021/la981598f, 10.1021/la981598f.
[15] R. Klajn, L. Fang, A. Coskun, M.A. Olson, P.J. Wesson, J.F. Stoddart, B. A. Grzybowski, Metal nanoparticles functionalized with molecular and supramolecular switches, J. Am. Chem. Soc. 131 (2009) 4233–4235. https://pubs.acs.org/doi/10.1021/ja9001585, 10.1021/ja9001585.
[16] L.M. Siewierski, W.J. Brittain, S. Petrash, M.D. Foster, Photoresponsive monolayers containing in-chain azobenzene, Langmuir 12 (1996) 5838–5844. https://pubs.acs.org/doi/10.1021/la960506o, 10.1021/la960506o.
[17] C.S. Diercks, O.M. Yaghi, The atom, the molecule, and the covalent organic framework, Science 355 (2017) eaal1585. https://www.science.org/doi/10.1126/science.aal1585, 10.1126/science.aal1585

[18] H. Furukawa, K.E. Cordova, M. O'Keeffe, O.M. Yaghi, The chemistry and applications of metal-organic frameworks, Science 341 (2013), 1230444. https://www.science.org/doi/10.1126/science.1230444, 10.1126/science.1230444.

[19] L. Sun, Y.A. Diaz-Fernandez, T.A. Gschneidtner, F. Westerlund, S. Lara-Avila, K. Moth-Poulsen, Single-molecule electronics: from chemical design to functional devices, Chem. Soc. Rev. 43 (2014) 7378–7411. http://xlink.rsc.org/?DOI=C4CS00143E, 10.1039/C4CS00143E.

[20] P. Tegeder, Optically and thermally induced molecular switching processes at metal surfaces, J. Phys. Condens. Matter 24 (2012), 394001. https://iopscience.iop.org/article/10.1088/0953-8984/24/39/394001, 10.1088/0953-8984/24/39/394001.

[21] R. Klajn, Immobilized azobenzenes for the construction of photoresponsive materials, Pure Appl. Chem. 82 (2010) 2247–2279. https://www.degruyter.com/document/doi/10.1351/PAC-CON-10-09-04/html, 10.1351/PAC-CON-10-09-04.

[22] B.K. Pathem, S.A. Claridge, Y.B. Zheng, P.S. Weiss, Molecular switches and motors on surfaces, Annu. Rev. Phys. Chem. 64 (2013) 605–630. https://www.annualreviews.org/doi/10.1146/annurev-physchem-040412-110045, 10.1146/annurev-physchem-040412-110045.

[23] N. Katsonis, M. Lubomska, M.M. Pollard, B.L. Feringa, P. Rudolf, Synthetic light-activated molecular switches and motors on surfaces, Prog. Surf. Sci. 82 (2007) 407–434. https://www.sciencedirect.com/science/article/pii/S0079681607000330?via%3Dihub, 10.1016/j.progsurf.2007.03.011.

[24] J. Zhang, Q. Zou, H. Tian, Photochromic materials: more than meets the eye, Adv. Mater. 25 (2013) 378–399. https://onlinelibrary.wiley.com/doi/10.1002/adma.201201521, 10.1002/adma.201201521.

[25] G. Bracco, in: B. Holst (Ed.), Surface Science Techniques, ume 51, Springer Berlin Heidelberg, 2013. http://link.springer.com/10.1007/978-3-642-34243-1, 10.1007/978-3-642-34243-1.

[26] S. Kobatake, S. Takami, H. Muto, T. Ishikawa, M. Irie, Rapid and reversible shape changes of molecular crystals on photoirradiation, Nature 446 (2007) 778–781. http://www.nature.com/articles/nature05669, 10.1038/nature05669.

[27] A. Fujimoto, N. Fujinaga, R. Nishimura, E. Hatano, L. Kono, A. Nagai, A. Sekine, Y. Hattori, Y. Kojima, N. Yasuda, M. Morimoto, S. Yokojima, S. Nakamura, B. L. Feringa, K. Uchida, Photoinduced swing of a diarylethene thin broad sword shaped crystal: a study on the detailed mechanism, Chem. Sci. 11 (2020) 12307–12315. https://pubs.rsc.org/en/content/articlelanding/2020/SC/D0SC05388K, 10.1039/D0SC05388K.

[28] J.J.D. de Jong, W.R. Browne, M. Walko, L.N. Lucas, L.J. Barrett, J.J. McGarvey, J. H. van Esch, B.L. Feringa, Raman scattering and ft-ir spectroscopic studies on dithienylethene switches—towards non-destructive optical readout, Org. Biomol. Chem. 4 (2006) 2387–2392. http://xlink.rsc.org/?DOI=B603914F, 10.1039/B603914F.

[29] N.J. Turro, V. Ramamurthy, J.C. Scaiano, Modern Molecular Photochemistry of Organic Molecules, University Science Books, 2010.

[30] W. Danowski, T. van Leeuwen, S. Abdolahzadeh, D. Roke, W.R. Browne, S. J. Wezenberg, B.L. Feringa, Unidirectional rotary motion in a metal–organic framework, Nat. Nanotechnol. 14 (2019) 488–494. http://www.nature.com/articles/s41565-019-0401-6, 10.1038/s41565-019-0401-6.

[31] W. Danowski, F. Castiglioni, A.S. Sardjan, S. Krause, L. Pfeifer, D. Roke, A. Comotti, W.R. Browne, B.L. Feringa, Visible-light-driven rotation of molecular motors in a dual-function metal–organic framework enabled by energy transfer, J. Am. Chem. Soc. 142 (2020) 9048–9056. https://pubs.acs.org/doi/10.1021/jacs.0c03063, 10.1021/jacs.0c03063.

[32] R. Feringa, H.S. Siebe, W.J.N. Klement, J.D. Steen, W.R. Browne, Single wavelength colour tuning of spiropyran and dithienylethene based photochromic coatings, Mater. Adv. 3 (2022) 282–289. http://xlink.rsc.org/?DOI=D1MA00839K, 10.1039/D1MA00839K.

[33] M. Kubista, R. Sjöback, S. Eriksson, B. Albinsson, Experimental correction for the inner-filter effect in fluorescence spectra, Analyst 119 (1994) 417–419. http://xlink.rsc.org/?DOI=AN9941900417, 10.1039/AN9941900417.

[34] R.L. McCreery, Raman Spectroscopy for Chemical Analysis, John Wiley & Sons, Inc., 2000. https://onlinelibrary.wiley.com/doi/book/10.1002/0471721646, 10.1002/0471721646.

[35] C. Stähler, L. Grunenberg, M.W. Terban, W.R. Browne, D. Doellerer, M. Kathan, M. Etter, B.V. Lotsch, B.L. Feringa, S. Krause, Light-driven molecular motors embedded in covalent organic frameworks, Chem. Sci. 13 (2022) 8253–8264. https://pubs.rsc.org/en/content/articlehtml/2022/sc/d2sc02282f. https://pubs.rsc.org/en/content/articlelanding/2022/sc/d2sc02282f, 10.1039/D2SC02282F.

[36] O. Ivashenko, J. van Herpt, B. Feringa, W. Browne, P. Rudolf, Rapid reduction of self-assembled monolayers of a disulfide terminated para-nitrophenyl alkyl ester on roughened au surfaces during xps measurements, Chem. Phys. Lett. 559 (2013) 76–81. https://www.sciencedirect.com/science/article/pii/S0009261413000122?via%3Dihub, 10.1016/j.cplett.2012.12.060.

[37] C.F. Bohren, D.R. Huffman, Absorption and Scattering of Light by Small Particles, John Wiley & Sons, Inc., 1998, https://doi.org/10.1002/9783527618156.

[38] J. Areephong, W.R. Browne, N. Katsonis, B.L. Feringa, Photo- and electrochromism of diarylethene modified ito electrodes—towards molecular based read–write–erase information storage, Chem. Commun. (2006) 3930–3932. https://pubs.rsc.org/en/content/articlelanding/2006/CC/B608502D, 10.1039/B608502D.

[39] L.-Q. Zheng, S. Yang, J. Lan, L. Gyr, G. Goubert, H. Qian, I. Aprahamian, R. Zenobi, Solution phase and surface photoisomerization of a hydrazone switch with a long thermal half-life, J. Am. Chem. Soc. 141 (2019) 17637–17645. https://pubs.acs.org/doi/10.1021/jacs.9b07057, 10.1021/jacs.9b07057.

[40] N.R. Krekiehn, M. Müller, U. Jung, S. Ulrich, R. Herges, O.M. Magnussen, Uv/vis spectroscopy studies of the photoisomerization kinetics in self-assembled azobenzene-containing adlayers, Langmuir 31 (2015) 8362–8370. https://pubs.acs.org/doi/10.1021/acs.langmuir.5b01645, 10.1021/acs.langmuir.5b01645.

[41] T.R. Rusch, A. Schlimm, N.R. Krekiehn, B.M. Flöser, F. Röhricht, M. Hammerich, I. Lautenschläger, T. Strunskus, R. Herges, F. Tuczek, O.M. Magnussen, Ordered adlayers of a combined lateral switch and rotor, J. Phys. Chem. C 123 (2019) 13720–13730. https://pubs.acs.org/doi/10.1021/acs.jpcc.9b02469, 10.1021/acs.jpcc.9b02469.

[42] Q. Chen, J. Sun, P. Li, I. Hod, P.Z. Moghadam, Z.S. Kean, R.Q. Snurr, J.T. Hupp, O. K. Farha, J.F. Stoddart, A redox-active bistable molecular switch mounted inside a metal–organic framework, J. Am. Chem. Soc. 138 (2016) 14242–14245. https://pubs.acs.org/doi/10.1021/jacs.6b09880, 10.1021/jacs.6b09880.

[43] J.P. Hopwood, J.W. Ciszek, Solid state and surface effects in thin-film molecular switches, Photochem. Photobiol. Sci. 16 (2017) 1095–1102. http://xlink.rsc.org/?DOI=C7PP00022G, 10.1039/C7PP00022G.

[44] H. Jacob, S. Ulrich, U. Jung, S. Lemke, T. Rusch, C. Schütt, F. Petersen, T. Strunskus, O. Magnussen, R. Herges, F. Tuczek, Monitoring the reversible photoisomerization of an azobenzene-functionalized molecular triazatriangulene platform on au(111) by irras, Phys. Chem. Chem. Phys. 16 (2014) 22643–22650. http://xlink.rsc.org/?DOI=C4CP03438D, 10.1039/C4CP03438D.

[45] K. Müller, J. Wadhwa, J.S. Malhi, L. Schöttner, A. Welle, H. Schwartz, D. Hermann, U. Ruschewitz, L. Heinke, Photoswitchable nanoporous films by loading azobenzene in metal–organic frameworks of type hkust-1, Chem. Commun. 53 (2017) 8070–8073. http://xlink.rsc.org/?DOI=C7CC00961E, 10.1039/C7CC00961E.

[46] Z. Wang, A. Knebel, S. Grosjean, D. Wagner, S. Bräse, C. Wöll, J. Caro, L. Heinke, Tunable molecular separation by nanoporous membranes, Nat. Commun. 7 (2016), 13872. http://www.nature.com/articles/ncomms13872, 10.1038/ncomms13872.

[47] H.A. Schwartz, M. Werker, C. Tobeck, R. Christoffels, D. Schaniel, S. Olthof, K. Meerholz, H. Kopacka, H. Huppertz, U. Ruschewitz, Novel photoactive spirooxazine based switch@mof composite materials, ChemPhotoChem 4 (2020) 195–206. https://onlinelibrary.wiley.com/doi/abs/10.1002/cptc.201900193, 10.1002/cptc.201900193.

[48] J. Lindon, G.E. Tranter, D. Koppenaal (Eds.), Infrared and Raman Spectroscopy of Minerals and Inorganic Materials, third ed., Academic Press, 2016 https://doi.org/10.1016/B978-0-12-409547-2.12154-7.

[49] M. Milosevic, Internal Reflection and ATR Spectroscopy, John Wiley & Sons, Inc., 2012. https://onlinelibrary.wiley.com/doi/book/10.1002/9781118309742, 10.1002/9781118309742.

[50] N.P.O. Ab, The Nobel Prize in Chemistry 2014 - nobelprize.Org, 2022. https://www.nobelprize.org/prizes/chemistry/2014/summary/. (Accessed 19 February 2022). accessed.

[51] A.C. Coleman, J. Areephong, J. Vicario, A. Meetsma, W.R. Browne, B.L. Feringa, In situ generation of wavelength-shifting donor-acceptor mixed-monolayer-modified surfaces, Angew. Chem. Int. Ed. 49 (2010) 6580–6584, https://doi.org/10.1002/anie.201002939, wiley.com/10.1002/anie.201002939.

[52] E. Smith, G. Dent, Modern Raman Spectroscopy: A Practical Approach, Wiley, 2019. https://onlinelibrary.wiley.com/doi/book/10.1002/9781119440598, 10.1002/9781119440598.

[53] W.R. Browne, T. Kudernac, N. Katsonis, J. Areephong, J. Hjelm, B.L. Feringa, Electro- and photochemical switching of dithienylethene self-assembled monolayers on gold electrodes, J. Phys. Chem. C 112 (2008) 1183–1190. https://pubs.acs.org/doi/10.1021/jp0766508, 10.1021/jp.0766508.

[54] T.C. Pijper, T. Kudernac, W.R. Browne, B.L. Feringa, Effect of immobilization on gold on the temperature dependence of photochromic switching of dithienylethenes, J. Phys. Chem. C 117 (2013) 17623–17632. https://pubs.acs.org/doi/10.1021/jp404925m, 10.1021/jp404925m.

[55] O. Ivashenko, J.T. van Herpt, B.L. Feringa, P. Rudolf, W.R. Browne, Uv/vis and nir light-responsive spiropyran self-assembled monolayers, Langmuir 29 (2013) 4290–4297. http://pubs.acs.org/doi/10.1021/la400192c, 10.1021/la400192c.

[56] Andor, Obtaining Raman spectra in nir using ingaas detectors. https://andor.oxinst.com/learning/view/article/raman-in-nir. (Accessed 14 February 2022) accessed.

[57] W.R. Browne, A. Draksharapu, E. Illy, Using the Full Spectrum for Raman: from Uv to Nir, Applied Spectroscopy, 2014, p. 16. https://www.spectroscopyonline.com/view/using-full-spectrum-raman-uv-nir-0.

[58] O. Ivashenko, J.T. van Herpt, B.L. Feringa, P. Rudolf, W.R. Browne, Electrochemical write and read functionality through oxidative dimerization of spiropyran self-assembled monolayers on gold, J. Phys. Chem. C 117 (2013) 18567–18577. http://pubs.acs.org/doi/10.1021/jp406458a, 10.1021/jp406458a.

[59] L. Kortekaas, W.R. Browne, Solvation dependent redox-gated fluorescence emission in a diarylethene-based sexithiophene polymer film, Adv. Opt. Mater. 4 (2016) 1378–1384, https://doi.org/10.1002/adom.201600330, wiley.com/10.1002/adom.201600330.

[60] D. Unjaroen, M. Swart, W.R. Browne, Electrochemical polymerization of iron(iii) polypyridyl complexes through c-c coupling of redox non-innocent phenolato ligands, Inorg. Chem. 56 (2017) 470–479. http://pubs.acs.org/doi/abs/10.1021/acs.inorgchem.6b02378, 10.1021/acs.inorgchem.6b02378.

[61] W.R. Browne, Resonance Raman Spectroscopy and its Application in Bioinorganic Chemistry, second ed., Elsevier, 2020, pp. 275–324. https://www.sciencedirect.com/science/article/pii/B9780444642257000080, 10.1016/B978-0-444-64225-7.00008-0.

[62] J. Langer, D.J. de Aberasturi, J. Aizpurua, R.A. Alvarez-Puebla, B. Auguié, J. J. Baumberg, G.C. Bazan, S.E.J. Bell, A. Boisen, A.G. Brolo, J. Choo, D. Cialla-May, V. Deckert, L. Fabris, K. Faulds, F.J.G. de Abajo, R. Goodacre, D. Graham, A. J. Haes, C.L. Haynes, C. Huck, T. Itoh, M. Käll, J. Kneipp, N.A. Kotov, H. Kuang, E. C.L. Ru, H.K. Lee, J.-F. Li, X.Y. Ling, S.A. Maier, T. Mayerhöfer, M. Moskovits, K. Murakoshi, J.-M. Nam, S. Nie, Y. Ozaki, I. Pastoriza-Santos, J. Perez-Juste, J. Popp, A. Pucci, S. Reich, B. Ren, G.C. Schatz, T. Shegai, S. Schlücker, L.-L. Tay, K.G. Thomas, Z.-Q. Tian, R.P.V. Duyne, T. Vo-Dinh, Y. Wang, K.A. Willets, C. Xu, H. Xu, Y. Xu, Y.S. Yamamoto, B. Zhao, L.M. Liz-Marzán, Present and future of surface-enhanced Raman scattering, ACS Nano 14 (2020) 28–117. https://pubs.acs.org/doi/10.1021/acsnano.9b04224, 10.1021/acsnano.9b04224.

[63] T. Schmid, L. Opilik, C. Blum, R. Zenobi, Nanoscale chemical imaging using tip-enhanced Raman spectroscopy: a critical review, Angew. Chem. Int. Ed. 52 (2013) 5940–5954. https://onlinelibrary.wiley.com/doi/10.1002/anie.201203849, 10.1002/anie.201203849.

[64] T. Deckert-Gaudig, A. Taguchi, S. Kawata, V. Deckert, Tip-enhanced Raman spectroscopy – from early developments to recent advances, Chem. Soc. Rev. 46 (2017) 4077–4110. https://pubs.rsc.org/en/content/articlelanding/2017/cs/c7cs00209b, 10.1039/C7CS00209B.

[65] E.A. Sprague-Klein, B. Negru, L.R. Madison, S.C. Coste, B.K. Rugg, A.M. Felts, M. O. McAnally, M. Banik, V.A. Apkarian, M.R. Wasielewski, M.A. Ratner, T. Seideman, G.C. Schatz, R.P.V. Duyne, Photoinduced plasmon-driven chemistry in trans-1,2-bis(4-pyridyl)ethylene gold nanosphere oligomers, J. Am. Chem. Soc. 140 (2018) 10583–10592. https://pubs.acs.org/doi/10.1021/jacs.8b06347, 10.1021/jacs.8b06347.

[66] Y. Fang, N.-H. Seong, D.D. Dlott, Measurement of the distribution of site enhancements in surface-enhanced Raman scattering, Science 321 (2008) 388–392. www.sciencemag.org/cgi/content/full/321/5887/385/DC1, 10.1126/science.1159499.

[67] L.-Q. Zheng, X. Wang, F. Shao, M. Hegner, R. Zenobi, Nanoscale chemical imaging of reversible photoisomerization of an azobenzene-thiol self-assembled monolayer by tip-enhanced Raman spectroscopy, Angew. Chem. Int. Ed. 57 (2018) 1025–1029, https://doi.org/10.1002/anie.201710443, wiley.com/10.1002/anie.201710443.

[68] N. Tallarida, L. Rios, V.A. Apkarian, J. Lee, Isomerization of one molecule observed through tip-enhanced Raman spectroscopy, Nano Lett. 15 (2015) 6386–6394. https://pubs.acs.org/doi/10.1021/acs.nanolett.5b01543, 10.1021/acs.nanolett.5b01543.

[69] H.-K. Choi, K.S. Lee, H.-H. Shin, J.-J. Koo, G.J. Yeon, Z.H. Kim, Single-molecule surface-enhanced Raman scattering as a probe of single-molecule surface reactions: promises and current challenges, Acc. Chem. Res. 52 (2019) 3008–3017. https://pubs.acs.org/doi/10.1021/acs.accounts.9b00358, 10.1021/acs.accounts.9b00358.

[70] M.D. Sonntag, D. Chulhai, T. Seideman, L. Jensen, R.P.V. Duyne, The origin of relative intensity fluctuations in single-molecule tip-enhanced Raman spectroscopy, J. Am. Chem. Soc. 135 (2013) 17187–17192. https://pubs.acs.org/doi/10.1021/ja408758j, 10.1021/ja408758j.

[71] H. Conrad, M.E. Kordesch, High Resolution Electron Energy Loss Spectroscopy, Applications, third ed., Elsevier, 2017, pp. 47–57. https://www.sciencedirect.com/science/article/pii/B9780128032244003472?via%3Dihub, 10.1016/B978-0-12-803224-4.00347-2.

[72] R. Azzam, N. Bashara, Ellipsometry and Polarized Light, 1987. North-Holland.

[73] D.K. Gramotnev, S.I. Bozhevolnyi, Plasmonics beyond the diffraction limit, Nat. Photonics 4 (2010) 83–91. https://www.nature.com/articles/nphoton.2009.282, 10.1038/nphoton.2009.282.

[74] G. Félix, K. Abdul-Kader, T. Mahfoud, I.A. Gural'skiy, W. Nicolazzi, L. Salmon, G. Molnár, A. Bousseksou, Surface plasmons reveal spin crossover in nanometric layers, J. Am. Chem. Soc. 133 (2011) 15342–15345. https://pubs.acs.org/doi/10.1021/ja207196b, 10.1021/ja207196b.

[75] R.W. Boyd, Nonlinear Optics, fourth ed., Academic Press, 2020.

[76] S.A. Shah, S. Baldelli, Chemical imaging of surfaces with sum frequency generation vibrational spectroscopy, Acc. Chem. Res. 53 (2020) 1139–1150. https://pubs.acs.org/doi/10.1021/acs.accounts.0c00057, 10.1021/acs.accounts.0c00057.

[77] T.A. Darwish, Y. Tong, M. James, T.L. Hanley, Q. Peng, S. Ye, Characterizing the photoinduced switching process of a nitrospiropyran self-assembled monolayer using in situ sum frequency generation spectroscopy, Langmuir 28 (2012) 13852–13860. https://pubs.acs.org/doi/10.1021/la302204f, 10.1021/la302204f.

[78] S. Wagner, F. Leyssner, C. Kördel, S. Zarwell, R. Schmidt, M. Weinelt, K. Rück-Braun, M. Wolf, P. Tegeder, Reversible photoisomerization of an azobenzene-functionalized self-assembled monolayer probed by sum-frequency generation vibrational spectroscopy, Phys. Chem. Chem. Phys. 11 (2009) 6242–6248. https://pubs.rsc.org/en/content/articlelanding/2009/cp/b823330f, 10.1039/b823330f.

[79] T. Garling, Y. Tong, T.A. Darwish, M. Wolf, R.K. Campen, The influence of surface potential on the optical switching of spiropyran self assembled monolayers, J. Phys. Condens. Matter 29 (2017), 414002, https://doi.org/10.1088/1361-648X/aa8118, 10.1088/1361-648X/aa8118.

[80] M. Schulze, M. Utecht, A. Hebert, K. Rück-Braun, P. Saalfrank, P. Tegeder, Reversible photoswitching of the interfacial nonlinear optical response, J. Phys. Chem. Lett. 6 (2015) 505–509. https://pubs.acs.org/doi/10.1021/jz502477m, 10.1021/jz502477m.

[81] C. Bronner, G. Schulze, K.J. Franke, J.I. Pascual, P. Tegeder, Switching ability of nitro-spiropyran on au(111): electronic structure changes as a sensitive probe during a ring-opening reaction, J. Phys. Condens. Matter 23 (2011), 484005. https://iopscience.iop.org/article/10.1088/0953-8984/23/48/484005, 10.1088/0953-8984/23/48/484005.

[82] S. Hagström, C. Nordling, K. Siegbahn, Electron spectroscopic determination of the chemical valence state, Z. Phys. 178 (1964) 439–444. http://link.springer.com/10.1007/BF01379473, 10.1007/BF01379473.

[83] G. Greczynski, L. Hultman, X-ray photoelectron spectroscopy: towards reliable binding energy referencing, Prog. Mater. Sci. 107 (2020), 100591. https://www.sciencedirect.com/science/article/pii/S0079642519300738?via%3Dihub, 10.1016/j.pmatsci.2019.100591.

[84] PHI, X-Ray Photoelectron Spectroscopy (Xps) Surface Analysis Technique, 2022. https://www.phi.com/surface-analysis-techniques/xps-esca.html. (Accessed 19 February 2022). accessed.

[85] J. Yano, V.K. Yachandra, X-ray absorption spectroscopy, Photosynth. Res. 102 (2009) 241–254. https://link.springer.com/article/10.1007/s11120-009-9473-8, 10.1007/s11120-009-9473-8.

[86] J. Stöhr, NEXAFS Spectroscopy, ume 25, Springer, 1996. http://link.springer.com/10.1007/978-3-662-02853-7, 10.1007/978-3-662-02853-7.

[87] T. Heinrich, C.H.-H. Traulsen, M. Holzweber, S. Richter, V. Kunz, S.K. Kastner, S. O. Krabbenborg, J. Huskens, W.E.S. Unger, C.A. Schalley, Coupled molecular switching processes in ordered mono- and multilayers of stimulus-responsive rotaxanes on gold surfaces, J. Am. Chem. Soc. 137 (2015) 4382–4390. https://pubs.acs.org/doi/10.1021/ja512654d, 10.1021/ja512654d.

[88] E. Ludwig, T. Strunskus, S. Hellmann, A. Nefedov, C. Wöll, L. Kipp, K. Rossnagel, Electronic structure, adsorption geometry, and photoswitchability of azobenzene layers adsorbed on layered crystals, Phys. Chem. Chem. Phys. 15 (2013), 20272. https://pubs.rsc.org/en/content/articlehtml/2013/cp/c3cp53003e, 10.1039/c3cp53003e.

[89] T. Weidner, F. Bretthauer, N. Ballav, H. Motschmann, H. Orendi, C. Bruhn, U. Siemeling, M. Zharnikov, Correlation between the molecular structure and photoresponse in aliphatic self-assembled monolayers with azobenzene tailgroups, Langmuir 24 (2008) 11691–11700. https://pubs.acs.org/doi/10.1021/la802454w, 10.1021/la802454w.

[90] A. Nilsson, L.G.M. Pettersson, Chemical bonding on surfaces probed by x-ray emission spectroscopy and density functional theory, Surf. Sci. Rep. 55 (2004) 49–167. https://www.sciencedirect.com/science/article/pii/S0167572904000573?via%3Dihub, 10.1016/j.surfrep.2004.06.002.

[91] U. Bergmann, P. Glatzel, X-ray emission spectroscopy, Photosynth. Res. 102 (2009) 255–266. https://link.springer.com/article/10.1007/s11120-009-9483-6, 10.1007/s11120-009-9483-6.

[92] T. Udayabhaskararao, P.K. Kundu, J. Ahrens, R. Klajn, Reversible photoisomerization of spiropyran on the surfaces of au25 nanoclusters, ChemPhysChem 17 (2016) 1805–1809, https://doi.org/10.1002/cphc.201500897, wiley.com/10.1002/cphc.201500897.

[93] R.A. van Delden, M.K.J. ter Wiel, M.M. Pollard, J. Vicario, N. Koumura, B. L. Feringa, Unidirectional molecular motor on a gold surface, Nature 437 (2005) 1337–1340. http://www.nature.com/articles/nature04127, 10.1038/nature04127.

[94] L.E. Marbella, Application of solid-state and in situ nmr to functional materials, Chem. Mater. 33 (2021) 8559–8561. https://pubs.acs.org/doi/10.1021/acs.chemmater.1c03113, 10.1021/acs.chemmater.1c03113.

[95] V.N. Vukotic, K.J. Harris, K. Zhu, R.W. Schurko, S.J. Loeb, Metal–organic frameworks with dynamic interlocked components, Nat. Chem. 4 (2012) 456–460. https://www.nature.com/articles/nchem.1354, 10.1038/nchem.1354.

[96] F. Nickel, M. Bernien, M. Herder, S. Wrzalek, P. Chittas, K. Kraffert, L.M. Arruda, L. Kipgen, D. Krüger, S. Hecht, W. Kuch, Light-induced photoisomerization of a diarylethene molecular switch on solid surfaces, J. Phys. Condens. Matter 29 (2017), 374001. https://iopscience.iop.org/article/10.1088/1361-648X/aa7c57, 10.1088/1361-648X/aa7c57.

[97] C. Gahl, D. Brete, F. Leyssner, M. Koch, E.R. McNellis, J. Mielke, R. Carley, L. Grill, K. Reuter, P. Tegeder, M. Weinelt, Coverage- and temperature-controlled isomerization of an imine derivative on au(111), J. Am. Chem. Soc. 135 (2013) 4273–4281. https://pubs.acs.org/doi/10.1021/ja309330e, 10.1021/ja309330e.

[98] C. Cocchi, T. Moldt, C. Gahl, M. Weinelt, C. Draxl, Optical properties of azobenzene-functionalized self-assembled monolayers: intermolecular coupling and many-body interactions, J. Chem. Phys. 145 (2016), 234701. http://aip.scitation.org/doi/10.1063/1.4971436, 10.1063/1.4971436.

[99] C. Cocchi, C. Draxl, Understanding the effects of packing and chemical terminations on the optical excitations of azobenzene-functionalized self-assembled monolayers, J. Phys. Condens. Matter 29 (2017), 394005. https://iopscience.iop.org/article/10.1088/1361-648X/aa7ca7, 10.1088/1361-648X/aa7ca7.

[100] G. Kresse, J. Furthmüller, Efficient iterative schemes for ab initio total-energy calculations using a plane-wave basis set, Phys. Rev. B 54 (1996) 11169–11186. https://link.aps.org/doi/10.1103/PhysRevB.54.11169, 10.1103/PhysRevB.54.11169.

[101] A.T. Zayak, Y.S. Hu, H. Choo, J. Bokor, S. Cabrini, P.J. Schuck, J.B. Neaton, Chemical Raman enhancement of organic adsorbates on metal surfaces, Phys. Rev. Lett. 106 (2011), 083003. https://journals.aps.org/prl/abstract/10.1103/PhysRevLett.106.083003, 10.1103/PhysRevLett.106.083003.

[102] T.A. Balema, N. Ulumuddin, C.J. Murphy, D.P. Slough, Z.C. Smith, R. T. Hannagan, N.A. Wasio, A.M. Larson, D.A. Patel, K. Groden, J.-S. McEwen, Y.-S. Lin, E.C.H. Sykes, Controlling molecular switching via chemical functionality: ethyl vs methoxy rotors, J. Phys. Chem. C 123 (2019) 23738–23746. https://pubs.acs.org/doi/full/10.1021/acs.jpcc.9b06664, 10.1021/acs.jpcc.9b06664.

[103] A.R. Kshirsagar, C. Attaccalite, X. Blase, J. Li, R. Poloni, Bethe-salpeter study of the optical absorption of trans and cis azobenzene-functionalized metal-organic

frameworks using molecular and periodic models, J. Phys. Chem. C 125 (2021) 7401–7412. https://pubs.acs.org/doi/10.1021/acs.jpcc.1c00367, 10.1021/acs.jpcc.1c00367.
[104] O. Ivashenko, H. Logtenberg, J. Areephong, A.C. Coleman, P.V. Wesenhagen, E. M. Geertsema, N. Heureux, B.L. Feringa, P. Rudolf, W.R. Browne, Remarkable stability of high energy conformers in self-assembled monolayers of a bistable electro- and photoswitchable overcrowded alkene, J. Phys. Chem. C 115 (2011) 22965–22975. https://pubs.acs.org/doi/10.1021/jp206889y, 10.1021/jp206889y.
[105] F. Nickel, M. Bernien, D. Krüger, J. Miguel, A.J. Britton, L.M. Arruda, L. Kipgen, W. Kuch, Highly efficient and bidirectional photochromism of spirooxazine on au (111), J. Phys. Chem. C 122 (2018) 8031–8036. https://pubs.acs.org/doi/10.1021/acs.jpcc.8b02220, 10.1021/acs.jpcc.8b02220.
[106] J. Mielke, F. Leyssner, M. Koch, S. Meyer, Y. Luo, S. Selvanathan, R. Haag, P. Tegeder, L. Grill, Imine derivatives on au(111): evidence for "inverted" thermal isomerization, ACS Nano 5 (2011) 2090–2097. https://pubs.acs.org/doi/10.1021/nn103297e, 10.1021/nn103297e.
[107] K.A. Willets, R.P.V. Duyne, Localized surface plasmon resonance spectroscopy and sensing, Annu. Rev. Phys. Chem. 58 (2007) 267–297. https://www.annualreviews.org/doi/10.1146/annurev.physchem.58.032806.104607, 10.1146/annurev.physchem.58.032806.104607.
[108] Z. Chu, Y. Han, T. Bian, S. De, P. Král, R. Klajn, Supramolecular control of azobenzene switching on nanoparticles, J. Am. Chem. Soc. 141 (2019) 1949–1960. https://pubs.acs.org/doi/10.1021/jacs.8b09638, 10.1021/jacs.8b09638.
[109] B.S. Zelakiewicz, A.C. de Dios, Tong, ^{13}C nmr spectroscopy of $^{13}C_1$-labeled octanethiol-protected au nanoparticles: shifts, relaxations, and particle-size effect, J. Am. Chem. Soc. 125 (2003) 18–19. https://pubs.acs.org/doi/10.1021/ja028302j, 10.1021/ja028302j.
[110] M.G. Berrettini, G. Braun, J.G. Hu, G.F. Strouse, Nmr analysis of surfaces and interfaces in 2-nm cdse, J. Am. Chem. Soc. 126 (2004) 7063–7070. https://pubs.acs.org/doi/10.1021/ja037228h, 10.1021/ja037228h.
[111] Y. Kim, D.D. Torres, P.K. Jain, Activation energies of plasmonic catalysts, Nano Lett. 16 (2016) 3399–3407. https://pubs.acs.org/doi/10.1021/acs.nanolett.6b01373, 10.1021/acs.nanolett.6b01373.
[112] A. Ulman, Formation and structure of self-assembled monolayers, Chem. Rev. 96 (1996) 1533–1554. https://pubs.acs.org/doi/10.1021/cr9502357, 10.1021/cr9502357.
[113] J.C. Love, L.A. Estroff, J.K. Kriebel, R.G. Nuzzo, G.M. Whitesides, Self-assembled monolayers of thiolates on metals as a form of nanotechnology, Chem. Rev. 105 (2005) 1103–1170. https://pubs.acs.org/doi/10.1021/cr0300789, 10.1021/cr0300789.
[114] M. Nakagawa, R. Watase, K. Ichimura, Preparation of monolayers of ion-paired macrocyclic amphiphiles to estimate a critical free space required for azobenzene photoisomerization, Chem. Lett. 28 (1999) 1209–1210. http://www.journal.csj.jp/doi/10.1246/cl.1999.1209, 10.1246/cl.1999.1209.
[115] H. Akiyama, K. Tamada, J. Nagasawa, K. Abe, T. Tamaki, Photoreactivity in self-assembled monolayers formed from asymmetric disulfides having para-substituted azobenzenes, J. Phys. Chem. B 107 (2003) 130–135. https://pubs.acs.org/doi/10.1021/jp026103g, 10.1021/jp026103g.
[116] C. Li, B. Ren, Y. Zhang, Z. Cheng, X. Liu, Z. Tong, A novel ferroceneylazobenzene self-assembled monolayer on an ito electrode: photochemical and electrochemical behaviors, Langmuir 24 (2008) 12911–12918. https://pubs.acs.org/doi/10.1021/la802101g, 10.1021/la802101g.
[117] A. Kunfi, R.B. Vlocskó, Z. Keresztes, M. Mohai, I. Bertóti, Ágnes Ábrahám, Éva Kiss, G. London, Photoswitchable macroscopic solid surfaces based on azobenzene-functionalized polydopamine/gold nanoparticle composite materials: formation, isomerization and ligand exchange, ChemPlusChem 85 (2020) 1–10. https://onlinelibrary.wiley.com/doi/abs/10.1002/cplu.201900674, 10.1002/cplu.201900674.
[118] M.S. Inkpen, Z. Liu, H. Li, L.M. Campos, J.B. Neaton, L. Venkataraman, Non-chemisorbed gold–sulfur binding prevails in self-assembled monolayers, Nat. Chem. 11 (2019) 351–358. http://www.nature.com/articles/s41557-019-0216-y, 10.1038/s41557-019-0216-y.
[119] H. Guesmi, N.B. Luque, E. Santos, F. Tielens, Does the s-h bond always break after adsorption of an alkylthiol on au(111)? Chem. Eur J. 23 (2017) 1402–1408, https://doi.org/10.1002/chem.201604574, wiley.com/10.1002/chem.201604574.
[120] G. Rajaraman, A. Caneschi, D. Gatteschi, F. Totti, A periodic mixed Gaussians–plane waves dft study on simple thiols on au(111): adsorbate species, surface reconstruction, and thiols functionalization, Phys. Chem. Chem. Phys. 13 (2011) 3886–3895. https://pubs.rsc.org/en/content/articlelanding/2011/cp/c0cp02042g, 10.1039/c0cp02042g.
[121] A. Tripathi, E.D. Emmons, S.D. Christesen, A.W. Fountain, J.A. Guicheteau, Kinetics and reaction mechanisms of thiophenol adsorption on gold studied by surface-enhanced Raman spectroscopy, J. Phys. Chem. C 117 (2013) 22834–22842. https://pubs.acs.org/doi/10.1021/jp407105v, 10.1021/jp407105v.
[122] F.P. Cometto, P. Paredes-Olivera, V.A. Macagno, E.M. Patrito, Density functional theory study of the adsorption of alkanethiols on cu(111), ag(111), and au(111) in the low and high coverage regimes, J. Phys. Chem. B 109 (2005) 21737–21748. https://pubs.acs.org/doi/10.1021/jp053273v, 10.1021/jp053273v.
[123] K.T. Carron, L.G. Hurley, Axial and azimuthal angle determination with surface-enhanced Raman spectroscopy: thiophenol on copper, silver, and gold metal surfaces, J. Phys. Chem. 95 (1991) 9979–9984. https://pubs.acs.org/doi/abs/10.1021/j100177a068, 10.1021/j100177a068.
[124] C.A. Szafranski, W. Tanner, P.E. Laibinis, R.L. Garrell, Surface-enhanced Raman spectroscopy of aromatic thiols and disulfides on gold electrodes, Langmuir 14 (1998) 3570–3579. https://pubs.acs.org/doi/10.1021/la9702502, 10.1021/la9702502.
[125] S. Li, D. Wu, X. Xu, R. Gu, Theoretical and experimental studies on the adsorption behavior of thiophenol on gold nanoparticles, J. Raman Spectrosc. 38 (2007) 1436–1443, https://doi.org/10.1002/jrs.1791, wiley.com/10.1002/jrs.1791.
[126] C.K.A. Nyamekye, S.C. Weibel, J.M. Bobbitt, E.A. Smith, Combined measurement of directional Raman scattering and surface-plasmon-polariton cone from adsorbates on smooth planar gold surfaces, Analyst 143 (2018) 400–408. https://pubs.rsc.org/en/content/articlelanding/2018/an/c7an01299c, 10.1039/C7AN01299C.
[127] C.K.A. Nyamekye, S.C. Weibel, E.A. Smith, Directional Raman scattering spectra of metal–sulfur bonds at smooth gold and silver substrates, J. Raman Spectrosc. 52 (2021) 1246–1255. https://analyticalsciencejournals.onlinelibrary.wiley.com/doi/full/10.1002/jrs.6124, 10.1002/jrs.6124.
[128] C.G.T. Feugmo, V. Liégeois, Analyzing the vibrational signatures of thiophenol adsorbed on small gold clusters by dft calculations, ChemPhysChem 14 (2013) 1633–1645. https://onlinelibrary.wiley.com/doi/full/10.1002/cphc.201201077, 10.1002/cphc.201201077.
[129] S.K. Saikin, Y. Chu, D. Rappoport, K.B. Crozier, A. Aspuru-Guzik, Separation of electromagnetic and chemical contributions to surface-enhanced Raman spectra on nanoengineered plasmonic substrates, J. Phys. Chem. Lett. 1 (2010) 2740–2746. https://pubs.acs.org/doi/full/10.1021/jz1008714, 10.1021/jz1008714.
[130] R.L. McCreery, A.J. Bergren, Progress with molecular electronic junctions: meeting experimental challenges in design and fabrication, Adv. Mater. 21 (2009) 4303–4322. https://onlinelibrary.wiley.com/doi/full/10.1002/adma.200802850 https://onlinelibrary.wiley.com/doi/abs/10.1002/adma.200802850 https://onlinelibrary.wiley.com/doi/10.1002/adma.200802850, 10.1002/ADMA.200802850.
[131] D. Roldan, V. Kaliginedi, S. Cobo, V. Kolivoska, C. Bucher, W. Hong, G. Royal, T. Wandlowski, Charge transport in photoswitchable dimethyldihydropyrene-type single-molecule junctions, J. Am. Chem. Soc. 135 (2013) 5974–5977. https://pubs.acs.org/doi/10.1021/ja401484j, 10.1021/ja401484j.
[132] N. Darwish, A.C. Aragonès, T. Darwish, S. Ciampi, I. Díez-Pérez, Multi-responsive photo- and chemo-electrical single-molecule switches, Nano Lett. 14 (2014) 7064–7070. https://pubs.acs.org/doi/10.1021/nl5034599, 10.1021/nl5034599.
[133] D. Stefani, K.J. Weiland, M. Skripnik, C. Hsu, M.L. Perrin, M. Mayor, F. Pauly, H. S.J. van der Zant, Large conductance variations in a mechanosensitive single-molecule junction, Nano Lett. 18 (2018) 5981–5988. https://pubs.acs.org/doi/10.1021/acs.nanolett.8b02810, 10.1021/acs.nanolett.8b02810.
[134] L. Meng, N. Xin, C. Hu, J. Wang, B. Gui, J. Shi, C. Wang, C. Shen, G. Zhang, H. Guo, S. Meng, X. Guo, Side-group chemical gating via reversible optical and electric control in a single molecule transistor, Nat. Commun. 10 (2019) 1450. http://www.nature.com/articles/s41467-019-09120-1, 10.1038/s41467-019-09120-1.
[135] M.C. Walkey, C.R. Peiris, S. Ciampi, A.C. Aragonès, R.B. Domínguez-Espíndola, D. Jago, T. Pulbrook, B.W. Skelton, A.N. Sobolev, I.D. Pérez, M.J. Piggott, G. A. Koutsantonis, N. Darwish, Chemically and mechanically controlled single-molecule switches using spiropyrans, ACS Appl. Mater. Interfaces 11 (2019) 36886–36894. https://pubs.acs.org/doi/10.1021/acsami.9b11044, 10.1021/acsami.9b11044.
[136] N. Xin, C. Hu, H.A. Sabea, M. Zhang, C. Zhou, L. Meng, C. Jia, Y. Gong, Y. Li, G. Ke, X. He, P. Selvanathan, L. Norel, M.A. Ratner, Z. Liu, S. Xiao, S. Rigaut, H. Guo, X. Guo, Tunable symmetry-breaking-induced dual functions in stable and photoswitched single-molecule junctions, J. Am. Chem. Soc. 143 (2021) 20811–20817. https://pubs-acs-org.proxy-ub.rug.nl/doi/full/10.1021/jacs.1c08997, 10.1021/jacs.1c08997.
[137] B. Xu, X. Xiao, N.J. Tao, Measurements of single-molecule electromechanical properties, J. Am. Chem. Soc. 125 (2003) 16164–16165. https://pubs.acs.org/doi/10.1021/ja038949j, 10.1021/ja038949j.
[138] B. Xu, N.J. Tao, Measurement of single-molecule resistance by repeated formation of molecular junctions, Science 301 (2003) 1221–1223. https://www.science.org/doi/10.1126/science.1087481, 10.1126/science.1087481.
[139] L. Kortekaas, J. Chen, D. Jacquemin, W.R. Browne, Proton-stabilized photochemically reversible e/z isomerization of spiropyrans, J. Phys. Chem. B 122 (2018) 6423–6430. http://pubs.acs.org/doi/10.1021/acs.jpcb.8b03528, 10.1021/acs.jpcb.8b03528.
[140] R.J. Nichols, W. Haiss, S.J. Higgins, E. Leary, S. Martin, D. Bethell, The experimental determination of the conductance of single molecules, Phys. Chem. Chem. Phys. 12 (2010) 2801–2815. http://xlink.rsc.org/?DOI=b922000c, 10.1039/b922000c.
[141] R.J. Nichols, S.J. Higgins, Single-molecule contacts exposed, Nat. Mater. 14 (2015) 465–466. https://www.nature.com/articles/nmat4225, 10.1038/nmat4225.
[142] B. Gui, Y. Meng, Y. Xie, K. Du, A.C. Sue, C. Wang, Immobilizing organic-based molecular switches into metal–organic frameworks: a promising strategy for switching in solid state, Macromol. Rapid Commun. 39 (2018), 1700388. https://onlinelibrary.wiley.com/doi/10.1002/marc.201700388, 10.1002/marc.201700388.
[143] Z. Wang, S. Grosjean, S. Bräse, L. Heinke, Photoswitchable adsorption in metal-organic frameworks based on polar guest-host interactions, ChemPhysChem 16 (2015) 3779–3783, https://doi.org/10.1002/cphc.201500829, wiley.com/10.1002/cphc.201500829.

[144] K. Müller, J. Helfferich, F. Zhao, R. Verma, A.B. Kanj, V. Meded, D. Bléger, W. Wenzel, L. Heinke, Switching the proton conduction in nanoporous, crystalline materials by light, Adv. Mater. 30 (2018), 1706551, https://doi.org/10.1002/adma.201706551 wiley.com/10.1002/adma.201706551.
[145] A.B. Kanj, A. Chandresh, A. Gerwien, S. Grosjean, S. Bräse, Y. Wang, H. Dube, L. Heinke, Proton-conduction photomodulation in spiropyran-functionalized mofs with large on–off ratio, Chem. Sci. 11 (2020) 1404–1410. http://xlink.rsc.org/?DOI=C9SC04926F, 10.1039/C9SC04926F.
[146] Z. Wang, K. Müller, M. Valášek, S. Grosjean, S. Bräse, C. Wöll, M. Mayor, L. Heinke, Series of photoswitchable azobenzene-containing metal-organic frameworks with variable adsorption switching effect, J. Phys. Chem. C 122 (2018) 19044–19050. https://pubs.acs.org/doi/10.1021/acs.jpcc.8b05843, 10.1021/acs.jpcc.8b05843.
[147] A.B. Kanj, J. Bürck, S. Grosjean, S. Bräse, L. Heinke, Switching the enantioselectivity of nanoporous host materials by light, Chem. Commun. 55 (2019) 8776–8779. https://pubs.rsc.org/en/content/articlelanding/2019/CC/C9CC02849H, 10.1039/C9CC02849H.
[148] S. Garg, H. Schwartz, M. Kozlowska, A.B. Kanj, K. Müller, W. Wenzel, U. Ruschewitz, L. Heinke, Conductance photoswitching of metal–organic frameworks with embedded spiropyran, Angew. Chem. Int. Ed. 58 (2019) 1193–1197, https://doi.org/10.1002/anie.201811458, wiley.com/10.1002/anie.201811458.
[149] W. Zhou, S. Grosjean, S. Bräse, L. Heinke, Thermal *cis*-to-*trans* isomerization of azobenzene side groups in metal-organic frameworks investigated by localized surface plasmon resonance spectroscopy, Z. Phys. Chem. 233 (2018) 15–22. https://www.degruyter.com/document/doi/10.1515/zpch-2017-1081/html, 10.1515/zpch-2017-1081.
[150] D.E. Williams, C.R. Martin, E.A. Dolgopolova, A. Swifton, D.C. Godfrey, O. A. Ejegbavwo, P.J. Pellechia, M.D. Smith, N.B. Shustova, Flipping the switch: fast photoisomerization in a confined environment, J. Am. Chem. Soc. 140 (2018) 7611–7622. https://pubs.acs.org/doi/10.1021/jacs.8b02994, 10.1021/jacs.8b02994.
[151] M. Klok, L.P.B.M. Janssen, W.R. Browne, B.L. Feringa, The influence of viscosity on the functioning of molecular motors, Faraday Discuss 143 (2009) 319–334. http://xlink.rsc.org/?DOI=b901841g, 10.1039/b901841g.
[152] S.M. Landge, E. Tkatchouk, D. Benítez, D.A. Lanfranchi, M. Elhabiri, W. A. Goddard, I. Aprahamian, Isomerization mechanism in hydrazone-based rotary switches: lateral shift, rotation, or tautomerization? J. Am. Chem. Soc. 133 (2011) 9812–9823. https://pubs.acs.org/doi/10.1021/ja200699v, 10.1021/ja200699v.
[153] I. Aprahamian, Hydrazone switches and things in between, Chem. Commun. 53 (2017) 6674–6684. https://pubs.rsc.org/en/content/articlelanding/2017/cc/c7cc02879b, 10.1039/C7CC02879B.
[154] H. Qian, S. Pramanik, I. Aprahamian, Photochromic hydrazone switches with extremely long thermal half-lives, J. Am. Chem. Soc. 139 (2017) 9140–9143. https://pubs.acs.org/doi/10.1021/jacs.7b04993, 10.1021/jacs.7b04993.
[155] X. Xie, D.G. Cahill, Thermometry of plasmonic nanostructures by anti-Stokes electronic Raman scattering, Appl. Phys. Lett. 109 (2016), 183104. https://aip.scitation.org/doi/abs/10.1063/1.4966289, 10.1063/1.4966289.
[156] W. Yang, J. Hulteen, G.C. Schatz, R.P.V. Duyne, A surface-enhanced hyper-Raman and surface-enhanced Raman scattering study of trans-1,2-bis(4-pyridyl)ethylene adsorbed onto silver film over nanosphere electrodes. vibrational assignments: experiment and theory, J. Chem. Phys. 104 (1996) 4313–4323. https://aip.scitation.org/doi/10.1063/1.471241, 10.1063/1.471241.
[157] S.L. Kleinman, B. Sharma, M.G. Blaber, A.-I. Henry, N. Valley, R.G. Freeman, M. J. Natan, G.C. Schatz, R.P.V. Duyne, Structure enhancement factor relationships in single gold nanoantennas by surface-enhanced Raman excitation spectroscopy, J. Am. Chem. Soc. 135 (2013) 301–308. https://pubs.acs.org/doi/10.1021/ja309300d, 10.1021/ja309300d.
[158] M. Banik, P.Z. El-Khoury, A. Nag, A. Rodriguez-Perez, N. Guarrottxena, G. C. Bazan, V.A. Apkarian, Surface-enhanced Raman trajectories on a nano-dumbbell: transition from field to charge transfer plasmons as the spheres fuse, ACS Nano 6 (2012) 10343–10354. https://pubs.acs.org/doi/10.1021/nn304277n, 10.1021/nn304277n.
[159] C.M. Aikens, L.R. Madison, G.C. Schatz, The effect of field gradient on sers, Nat. Photonics 7 (2013) 508–510. https://www.nature.com/articles/nphoton.2013.153, 10.1038/nphoton.2013.153.
[160] Y. Atassi, J.A. Delaire, K. Nakatani, Coupling between photochromism and second-harmonic generation in spiropyran- and spirooxazine-doped polymer films, J. Phys. Chem. 99 (1995) 16320–16326. https://pubs.acs.org/doi/10.1021/j100044a019, 10.1021/j100044a019.
[161] N. Tamaoki, E.V. Keuren, H. Matsuda, K. Hasegawa, T. Yamaoka, Photoreversible optical nonlinearities of polymeric films containing spiropyran with long alkyl chains, Appl. Phys. Lett. 69 (1996) 1188–1190. http://aip.scitation.org/doi/10.1063/1.117406, 10.1063/1.117406.
[162] N.D. Lai, W.L. Wang, J.H. Lin, C.C. Hsu, Optical manipulation of third-harmonic generation via either one- or two-photon excitation in diarylethene-polymethylmethacrylate polymer thin films, Appl. Phys. B 80 (2005) 569–572. http://link.springer.com/10.1007/s00340-004-1727-8, 10.1007/s00340-004-1727-8.
[163] D. Barriet, C.M. Yam, O.E. Shmakova, A.C. Jamison, T.R. Lee, 4-mercaptophenylboronic acid sams on gold: comparison with sams derived from thiophenol, 4-mercaptophenol, and 4-mercaptobenzoic acid, Langmuir 23 (2007) 8866–8875. https://pubs.acs.org/doi/10.1021/la7007733, 10.1021/la7007733.
[164] M. Willenbockel, R.J. Maurer, C. Bronner, M. Schulze, B. Stadtmüller, S. Soubatch, P. Tegeder, K. Reuter, F.S. Tautz, Coverage-driven dissociation of azobenzene on cu(111): a route towards defined surface functionalization, Chem. Commun. 51 (2015) 15324–15327. http://xlink.rsc.org/?DOI=C5CC05003K, 10.1039/C5CC05003K.
[165] M. Piantek, J. Miguel, A. Krüger, C. Navío, M. Bernien, D.K. Ball, K. Hermann, W. Kuch, Temperature, surface, and coverage-induced conformational changes of azobenzene derivatives on cu(001), J. Phys. Chem. C 113 (2009) 20307–20315. https://pubs.acs.org/doi/10.1021/jp907641f, 10.1021/jp907641f.